HHS Public Access

Author manuscript

Sci Transl Med. Author manuscript; available in PMC 2022 April 21.

Published in final edited form as:

Sci Transl Med. 2021 April 21; 13(590): . doi:10.1126/scitranslmed.abd6434.

The melanocortin-3 receptor is a pharmacological target for the regulation of anorexia

Patrick Sweeney[1,†], **Michelle N. Bedenbaugh**[2,†], **Jose Maldonado**[2], **Pauline Pan**[1], **Katelyn Fowler**[1], **Savannah Y. Williams**[1], **Luis E. Gimenez**[1], **Masoud Ghamari-Langroudi**[2], **Griffin Downing**[1,3], **Yijun Gui**[1,3], **Colleen K. Hadley**[1], **Stephen T. Joy**[1], **Anna K. Mapp**[1,4], **Richard B. Simerly**[2,*], **Roger D. Cone**[1,3,5,*]

[1]Life Sciences Institute, University of Michigan, Ann Arbor, MI 48109, USA.

[2]Department of Molecular Physiology and Biophysics, School of Medicine, Vanderbilt University, Nashville, TN 37240, USA.

[3]Department of Molecular, Cellular, and Developmental Biology, School of Literature, Science, and the Arts, University of Michigan, Ann Arbor, MI 48109, USA.

[4]Department of Chemistry, School of Literature, Science, and the Arts, University of Michigan, Ann Arbor, MI 48109, USA.

[5]Department of Molecular and Integrative Physiology, School of Medicine, University of Michigan, Ann Arbor, MI 48109, USA.

Abstract

Ablation of hypothalamic AgRP (Agouti-related protein) neurons is known to lead to fatal anorexia, whereas their activation stimulates voracious feeding and suppresses other motivational states including fear and anxiety. Despite the critical role of AgRP neurons in bidirectionally controlling feeding, there are currently no therapeutics available specifically targeting this circuitry. The melanocortin-3 receptor (MC3R) is expressed in multiple brain regions and exhibits sexual dimorphism of expression in some of those regions in both mice and humans. MC3R deletion produced multiple forms of sexually dimorphic anorexia that resembled aspects of human anorexia nervosa. However, there was no sexual dimorphism in the expression of MC3R in AgRP neurons, 97% of which expressed MC3R. Chemogenetic manipulation of arcuate MC3R neurons and pharmacologic manipulation of MC3R each exerted potent bidirectional regulation

*Corresponding author. rcone@umich.edu (R.D.C.); richard.simerly@vanderbilt. edu (R.B.S.).
†These authors contributed equally to this work.

Author contributions: P.S., M.N.B., J.M., P.P., K.F., S.Y.W., L.E.G., M.G.-L., G.D., Y.G., C.K.H., and S.T.J. conducted experiments. P.S., M.N.B., A.K.M., S.T.J., R.B.S., and R.D.C. designed experiments and analyzed data, P.S., M.N.B., R.B.S., and R.D.C. prepared the manuscript.

Competing interests: P.S., R.D.C., L.E.G., and S.Y.W. hold equity in Courage Therapeutics Inc. and are inventors of intellectual property optioned to Courage Therapeutics Inc. R.D.C. chairs the Scientific Advisory Board at Courage Therapeutics Inc. Patent PCT/US2020/038757, Targeting Melanocortin 3 Receptor for Treatment/Prevention of Eating, Metabolism, and/or Emotional Disorders, has been filed containing some of the findings in the manuscript.

SUPPLEMENTARY MATERIALS

stm.sciencemag.org/cgi/content/full/13/590/eabd6434/DC1

Materials and Methods

References (51, 52)

over feeding behavior in male and female mice, whereas global ablation of MC3R-expressing cells produced fatal anorexia. Pharmacological effects of MC3R compounds on feeding were dependent on intact AgRP circuitry in the mice. Thus, the dominant effect of MC3R appears to be the regulation of the AgRP circuitry in both male and female mice, with sexually dimorphic sites playing specialized and subordinate roles in feeding behavior. Therefore, MC3R is a potential therapeutic target for disorders characterized by anorexia, as well as a potential target for weight loss therapeutics.

INTRODUCTION

AgRP (Agouti-related protein) neurons reside exclusively in the arcuate nucleus (ARH) of the hypothalamus where they sense energy stores in adipose tissue (1, 2) via the direct and indirect action of the hormone leptin on these cells (3, 4). A decrease in leptin activates these GABA (γ-aminobutyric acid)–releasing (GABAergic) neurons (4, 5), which project to multiple regions involved in metabolic regulation and behavior, including other cell types in the ARH, paraventricular nucleus of the hypothalamus (PVN), ventral tegmental area, parabrachial nucleus, amygdala, nucleus accumbens, and paraventricular nucleus of the thalamus, resulting in both the stimulation of food intake (1, 6) and the suppression of competing motivational states, including anxiety, fear, and alarm (7–10). AgRP neurons are known to be essential for feeding behavior, because ablation of this small number of cells produces fatal anorexia (11); conversely, optogenetic (12) or chemogenetic (13) activation of these cells produces profound hyperphagia, even when animals are fully sated or confronted with stimuli producing anxiety or fear (8, 9). These data showing bidirectional control of feeding suggest that a pharmacological target for the control of AgRP circuitry might have utility both in obesity and disorders of anorexia such as anorexia nervosa, cancer anorexia, and aging anorexia. Despite the importance of AgRP neurons for feeding behavior and the potential pharmacological utility of compounds targeting AgRP circuitry, there are currently no approved therapeutics targeting this system.

We previously demonstrated that the melanocortin-3 receptor (MC3R) is expressed presynaptically in AgRP projections to melanocortin-4 receptor (MC4R) neurons in the PVN (14), where it acts to regulate the release of GABA from AgRP neurons onto MC4R target sites. The MC3R also appears to regulate GABA release from AgRP neurons onto proopiomelanocortin (POMC) cells in the ARH (15). However, the receptor is widely expressed in the central nervous system (CNS) (16) and was previously reported to be expressed in about 50% of both the orexigenic AgRP neurons and the anorexigenic POMC neurons of the ARH (17). Early reports using a melanocortin peptide agonist with 20 to 100× specificity for the MC3R versus MC4R were equivocal, with low doses stimulating food intake and higher doses inhibiting food intake (18). However, potent and specific MC3R agonists (19) and antagonists (20) have only recently been reported and have not yet been tested in vivo. Therefore, the net effect of MC3R activation or inhibition on feeding behavior and the specific cell types and circuits involved in MC3R-mediated effects on feeding are unknown.

Although some basic mapping of MC3R-positive cells has been reported (16), the neurochemical identity of MC3R neurons is largely unknown, and despite the role of the receptor at the intersection of sex/reproductive state and energy homeostasis (14, 21), nearly all of the reported neuroanatomy and physiology is from male animals. In this study, we characterized the distribution of MC3R cells by light-sheet microscopy and single-cell sequencing as well as the sexually dimorphic expression of the receptor in key hypothalamic nuclei and cell types using quantitative RNA fluorescence in situ hybridization (FISH). Using genetic, pharmacological, and in vivo imaging approaches, we examined the role of the MC3R in mouse models of anorexia and characterized the nonsexually dimorphic dominance of orexigenic ARH MC3R neurons in the bidirectional control of food intake.

RESULTS

MC3R expression is abundant and sexually dimorphic in discrete hypothalamic cell types

To evaluate the distribution of MC3R expression throughout the mouse hypothalamus, we used whole-brain tissue clearing and light-sheet imaging to visualize hypothalamic neurons labeled with Td-Tomato fluorescence through MC3R-Cre targeting. Analysis of the hypothalamus in optically cleared brains revealed at least a few distinctly labeled MC3R-positive neurons in each major region of the hypothalamus, rostrally extending from the preoptic region (Fig. 1, A to D) through premammillary regions of the hypothalamus (movie S1). However, dense clusters of MC3R-positive neurons were present in hypothalamic nuclei implicated previously in the regulation of food intake, including the ventromedial and dorsomedial hypothalamic nuclei. Particularly high densities of labeled neurons were located in the dorsomedial component of the ventromedial hypothalamic nucleus (Fig. 1D) and ARH, which contained a high density of labeled neurons throughout the rostrocaudal extent of the nucleus (Fig. 1, A, B, and D, and movie S2). *Mc3r* exhibited broader expression throughout the medial basal hypothalamus, whereas *Mc4r* expression was lower and more localized to the ventral-lateral region of the ventromedial hypothalamus (Fig. 1E).

Next, we used multiplex FISH to compare *Mc3r* expression in male and female mice. A number of notable sexual dimorphisms were apparent. First, *Mc3r* mRNA expression in the ARH in male mice was about twice (7731 ± 887 versus 4128 ± 460 spots) that observed in females, both in terms of overall abundance and in numbers of labeled cells (Fig. 1, F to H). Quantification of *Mc3r*-positive ARH neurons in male and female mice demonstrated that the difference resided entirely in an undefined set of non-*Pomc*, non-*Agrp* neurons expressing *Mc3r* (Fig. 1H). Because kisspeptin (*Kiss1*) neurons present in the ARH influence the reproductive neuroendocrine axis and may function differently in males and females (22), we reasoned that these neurons may be a portion of the undefined set of non-*Pomc*, non-*Agrp* neurons exhibiting sexually dimorphic expression of *Mc3r* in the ARH. We observed that a higher percentage of *Kiss1* neurons in males expressed *Mc3r* compared with females (Fig. 1, I and J). We also characterized *Mc3r* expression in a well-known sexually dimorphic hypothalamic nucleus, the anteroventral periventricular nucleus of the preoptic region (AVPV), and observed twice the amount (1624 ± 152 versus 827 ± 117 spots) of *Mc3r* mRNA in female mice compared with males (Fig. 1, K to L). To determine whether MC3R was also sexually dimorphic in humans, we examined the

GTEx (Genotype-Tissue Expression project) human transcriptomic dataset to measure male and female MC3R expression in the human hypothalamus. MC3R abundance exhibited a 300% increase in male versus female hypothalamus, indicating that MC3R exhibits sexually dimorphic expression patterns in the human hypothalamus (table S1). In contrast to MC3R, other human genes encoding the central melanocortin receptors and ligands exhibited only modest sexually dimorphic abundance in the GTEx dataset, suggesting that MC3R may exert a unique sexually dimorphic role within the human central melanocortin system (table S1).

Given the dense expression of *Mc3r* in the ARH and the importance of this region for regulating feeding, we next used multiplex FISH to quantitatively define *Mc3r* expression in the orexigenic *Agrp* neurons and the anorexigenic *Pomc* neurons located in the ARH. Consistent with previous findings, we found that *Mc3r* was expressed in both *Agrp* and *Pomc* neurons (16, 17) in addition to other cell types (Fig. 1M). However, *Mc3r* was expressed at a greater frequency and abundance in orexigenic *Agrp* neurons relative to anorexigenic *Pomc* neurons (Fig. 1, N to P). Whereas previous reports suggested that 50% of *Agrp* neurons expressed *Mc3r* (17), we found that about 97% of *Agrp* neurons contained *Mc3r* mRNA in both male and female mice (Fig. 1N). Furthermore, *Mc3r* mRNA was expressed at over twice the amount in *Agrp* neurons as in *Pomc* neurons (Fig. 1, O and P).

Although *Mc3r* was densely expressed in *Agrp* neurons, and *Pomc* neurons to a lesser degree, a large proportion of ARH *Mc3r* neurons did not express either *Agrp* or *Pomc*. To determine the identity of the other ARH cell populations expressing *Mc3r*, we analyzed the gene expression profile of the *Mc3r*-expressing cells in a previously published (23) ARH single-cell transcriptomic dataset. We identified 10 distinct clusters of *Mc3r*-expressing neurons in the ARH (figs. S1 and S2); *Kiss1* expression was primarily found in the *Tac2* cluster. Consistent with our previous data, two of these clusters were marked by *Agrp* expression, and one cluster was characterized as *Pomc*-expressing neurons (figs. S1 and S2). However, we also identified *Mc3r* expression in the recently characterized orexigenic non-*Agrp*, vGAT (*Slc32a1*)–expressing neurons (clusters 1, 3, 6, and 7; figs. S1 and S2) (24), the orexigenic tyrosine hydroxylase (*Th*)–expressing neurons (cluster 3; figs. S1 and S2) (25), and the recently characterized orexigenic *Pnoc* neurons (figs. S1 and S2) (26). *Mc3r* expression was also observed to a lesser degree in the anorexic ARH vGLUT2 (*Slc17a6*) neurons (27). Thus, in addition to dense expression in *Agrp* neurons, *Mc3r* expression was also observed in multiple distinct orexigenic cell types in the ARH.

Because single-cell approaches may only capture a portion of all ARH *Mc3r* neurons, we performed additional RNAscope FISH analysis to quantitatively determine *Mc3r* expression in the key orexigenic cell types in the ARH, including somatostatin (*Sst*), oxytocin receptor (*Oxtr*), *Th*, and *Slc32a1* neurons (fig. S3). We found that about 89% of *Sst*, 77% of *Oxtr*, 74% of *Th*, and 74% of *Slc32a1* neurons in the ARH expressed *Mc3r* (fig. S3). Thus, *Mc3r* is highly expressed in multiple orexigenic cell types in the ARH, and *Agrp* neurons exhibit the highest percentage of coexpression of *Mc3r*.

MC3R knockout mice exhibit enhanced anorexia and anxiety-like behavior

Because the central melanocortin system is well known to regulate feeding (1) and we found that MC3R exhibited sexually dimorphic expression within hypothalamic feeding and behavioral centers, we next sought to determine whether MC3R could have sexually dimorphic effects on feeding behavior. Given the observed sexual dimorphisms in the prevalence of neuropsychiatric eating disorders, we chose to examine the effects of MC3R on a variety of stress-induced anorexia paradigms in male versus female mice. First, we performed social-isolation anorexia experiments to evaluate anorexic behavior in response to the persistent psychological stressor of social isolation. No difference in food intake or body weight was observed between group-housed MC3R knockout (KO) and wild-type (WT) mice before social isolation (Fig. 2A). However, upon single housing, both male and female MC3R KO mice consumed comparably less food (Fig. 2, B to E) and lost more weight than WT littermate control mice (Fig. 2F).

Although we did not detect a sexually dimorphic effect in response to social-isolation anorexia, we did identify two assays in which deletion of the MC3R produced sexually dimorphic responses. First, in restraint stress–induced anorexia experiments, male MC3R KO mice consumed less food than WT mice and lost more body weight than WT littermates after a single acute restraint stress (Fig. 2, G and H). Furthermore, during continued daily restraint, male, but not female, MC3R KO mice displayed an enhanced stress-induced reduction in body weight (Fig. 2, I and J). We next performed novelty-suppressed feeding (NSF) assays in male and female MC3R KO and WT mice, in which animals fasted overnight are examined because they must enter into the center of an open field to consume a food pellet. This assay examines the interaction between hunger drive and a competing motivation state, the fear and anxiety resulting from entering into the center of the open field. We did not observe any differences in food-seeking or anxiety-related behavior in male mice, although a trend toward increased anxiety-related behavior was observed in male MC3R KO mice (Fig. 2, K to M). In contrast, female MC3R KO mice displayed a severe anxiety/ food avoidance phenotype characterized by reduced latency to enter the food zone, reduced time in the food zone, and reduced time eating (Fig. 2, K to N, and fig. S4). Furthermore, 80% of female MC3R KO mice exhibited aphagic episodes during testing, in contrast to only 7.7% of male mice (Fig. 2L), representing a sexually dimorphic form of anorexia like that observed in anorexia nervosa, in which 90% of cases are in females (28). These findings indicate that MC3R KO mice exhibit distinct sexually dimorphic anorexia phenotypes in both male and female mice, along with a nondimorphic anorexic response to social isolation.

To separately determine the contribution of MC3R signaling to hunger sensing and anxiety, respectively, we performed fast-induced refeeding experiments and anxiety-related behavior experiments in MC3R KO and WT mice. Consistent with the defective fast-induced refeeding observed in male MC3R KO mice (14), female MC3R KO mice displayed an impairment in fast-induced refeeding, with cumulative food intake and body weight gain remaining lower in the MC3R KO mice for multiple days after fasting (fig. S5). To determine whether MC3R KO mice displayed defective anxiety-related behavior in the absence of hunger or food-related perturbations, we next measured anxiety-related behavior

in male and female ad libitum–fed MC3R KO and WT mice. In the elevated plus maze (EPM) test of anxiety-related behavior, MC3R KO mice spent less time in the open arms and entered the open arms less frequently during testing (fig. S6, A to C). In the open-field test (OFT) of anxiety-related behavior, MC3R KO mice spent less time in the center and traveled less distance in the center of the open field, indicating increased anxiety-related behavior (fig. S6). However, we note that elevated basal anxiety in the EPM and OFT only achieved significance in male mice (fig. S6). Increased anxiety-related behavior was also observed in the EPM test in male mice for a second MC3R KO mouse strain (MC3R TB/TB; fig. S7). Therefore, MC3R KO mice display both defective hunger sensing and increased anxiety-related behavior.

ARH MC3R neurons bidirectionally regulate feeding and anxiety

Because we identified MC3R expression in multiple orexigenic and anorexigenic cell types (Fig. 1 and figs. S1 to S3), we next tested the net effect of MC3R-expressing neurons on feeding behavior by using a genetic approach to ablate MC3R-expressing cells in adult mice. To this end, we expressed the diphtheria toxin (DT) receptor in MC3R neurons by breeding MC3R-Cre mice to Rosa26-LSL-iDTR mice (MC3R-DTR mice). In response to DT treatment (50 μg/kg), we observed a reduction in body weight in both male and female mice (Fig. 3A). Male mice continued to lose weight out to 19 days after DT injection, at which point the experiment had to be terminated because of animal welfare concerns (Fig. 3A). At days 30 to 32, male mice that received DT lost 28% and female mice lost 11% of their original body weight (Fig. 3B); at that same time point, a ~50 and ~28% reduction in food intake was observed in male and female mice, respectively (Fig. 3C). Although MC3R is expressed in both orexigenic and anorexigenic cell types, these results resemble previous reports ablating AgRP neurons (11), suggesting that AgRP neurons exhibit a major role in communicating the downstream effects of MC3R. Although female MC3R neuron–ablated mice exhibited an anorexic response and lost weight after DT injection, female mice did not continue to lose weight after the first week of DT treatment; however, we did not quantitate the efficacy of MC3R neuronal ablation in these experiments. Therefore, despite MC3R expression in multiple brain regions and cell types, the net effect of MC3R neuron ablation largely resembles the starvation phenotype observed upon AgRP neuron ablation (11).

Our findings thus far, along with previous reports (18, 29), suggested that the net effect of MC3R neurons in both male and female mice may be to stimulate feeding. However, we also found a large population of non-AgRP, non-POMC, MC3R-expressing neurons in the ARH in other recently identified orexigenic ARH cell types, which may contribute to a potential feeding effect. Therefore, we used viral-mediated chemogenetic approaches to specifically manipulate the MC3R-containing neurons in the ARH by stereotaxically targeting an adeno-associated virus (AAV) viral vector expressing the DREADD (designer receptor exclusively activated by designer drugs) activator hM3Dq in a Cre-dependent manner to the ARH in MC3R-Cre mice (Fig. 4A; male and female mice are pooled in each experiment in Fig. 4 and figs. S9 and S10, unless otherwise indicated) (30). We observed dense Fos expression specifically in ARH-MC3R neurons after injections of the DREADD agonist clozapine *N*-oxide (CNO), indicating that the DREADD approach efficiently activated ARH-MC3R neurons (Fig. 4B). Consistent with previous acute experiments (14), chemogenetic activation

of ARH MC3R neurons robustly stimulated food intake, whereas chemogenetic inhibition of these neurons suppressed daily feeding (Fig. 4, C and D). Similar DREADD-mediated effects on feeding were observed in both male and female mice (fig. S8). To evaluate the long-term effects of manipulating ARH MC3R neurons, we injected CNO twice daily to mice (Fig. 4, E and F) transduced with hM3Dq or control mCherry virus in ARH MC3R neurons. Chronic stimulation of ARH MC3R neurons stimulated feeding and increased body weight (Fig. 4, E and F). However, continued CNO administration did not produce further increases in body weight beyond the first 3 days of treatment (Fig. 4F). Similar diminished effects of continued chemogenetic activation have been previously reported for ARH AgRP neurons, suggesting a limitation of chemogenetic activation approaches, perhaps due to receptor desensitization to CNO (13, 31). No change in food intake or body weight was observed after CNO injections in littermate control mice (fig. S9). We next used inhibitory DREADDs to selectively inhibit the activity of ARH-MC3R cells. Inhibition of ARH-MC3R neurons continuously reduced both food intake and body weight after twice daily administration of CNO for 4 days (Fig. 4, G and H); no effect on body weight was observed in WT-littermate control mice after CNO injections (Fig. 4H). Together, our results indicate that ARH-MC3R neurons can bidirectionally regulate both feeding and body weight.

Activation of AgRP neurons reduces anxiety-related behaviors (7, 32), whereas activation of POMC neurons has been reported to increase anxiety-related and aversive behaviors (33). Furthermore, MC3R KO mice exhibited enhanced anxiety-related behavior (figs. S6 and S7). Because we previously confirmed that activation of ARH-MC3R neurons increases feeding and body weight, we next tested whether selective activation or inhibition of ARH-MC3R neurons modulates anxiety-related behavior. In the EPM and OFT, acute chemogenetic activation of ARH-MC3R neurons increased both time in the open arms in the EPM test and time in the center in the OFT in both male and female mice, indicating reduced anxiety-related behavior (Fig. 4, I to K). No differences in locomotion were detected in the EPM or OFT after activation of ARH-MC3R neurons, indicating that the observed effects on anxiety-related behavior were not secondary to altered locomotion (fig. S10). We next examined anxiety-related behavior after selective inhibition of ARH-MC3R neurons using inhibitory DREADDs. In the EPM and OFT, inhibition of ARH-MC3R neurons reduced time spent in the open arms and time spent in the center, respectively, indicating increased anxiety-like behavior (Fig. 4, L to N). No differences in locomotion were detected in the EPM or OFT after inhibition of ARH-MC3R neurons, indicating that these changes were not secondary to changes in locomotion (fig. S10).

MC3R-specific agonists increase feeding and reduce anxiety in mice

Although ablation of MC3R-containing cells (Fig. 3) and collective regulation of ARH MC3R neurons using DREADDs (Fig. 4) both produced potent effects on feeding, MC3R is expressed in dozens of sites in the CNS (16) and in multiple ARH cell types, all of which may be presumably modulated by administration of MC3R-specific compounds. Thus, we sought to test whether pharmacological regulation of MC3R throughout the brain would recapitulate the feeding effects observed upon collective DREADD activation of all ARH MC3R neurons. Previously, the MC3R agonist D-Trp-8-γ–melanocyte-stimulating

hormone was shown to stimulate food intake at lower doses and inhibit food intake at higher doses (18); the latter response was shown to be mediated by the MC4R, resulting from the modest specificity of the peptide for the MC3R. Recently, more potent and specific MC3R compounds have been reported but not yet tested in vivo (19, 20), including a potent MC3R-specific antagonist (20). Administration of an MC3R-specific agonist, referred to here as compound 18 [C18; 5 μg, intracerebroventricularly (icv)] (19), produced profound hyperphagia, stimulating food intake by over 50% 6 hours after administration and increasing 24-hour food intake and body weight after a single injection (Fig. 5, A to C, and fig. S11; male mice are shown in Fig. 5 unless otherwise noted). Similar effects on feeding were observed in both male and female mice (fig. S12), and no effect on feeding was observed in MC3R KO mice treated with C18 (Fig. 5, D and E).

To determine how pharmacological stimulation of MC3R affects meal structure, energy expenditure, locomotion, and nutrient partitioning, we performed indirect calorimetry on a separate cohort of mice after acute intraperitoneal administration of C18. Consistent with previous findings, C18 administration increased food intake by increasing meal frequency (Fig. 5G); no difference in meal size was noted (Fig. 5H). Furthermore, no differences were detected in feed efficiency, energy expenditure, oxygen consumption, locomotion, or respiratory exchange ratio/nutrient partitioning after C18 administration (fig. S13). Melanocortin compounds have previously been shown to exhibit on-target pressor effects, and MC3R stimulation had no effect on heart rate, blood pressure, or activity as assessed by telemetry; however, we did note a transient decrease in heart rate and blood pressure in a subset of mice after C18 administration (fig. S14). We tested the effects of chronic MC3R stimulation on body weight by implanting subcutaneous mini pumps containing either vehicle or C18 (10 mg/kg per day for 6 days) into a cohort of WT mice. Mini-pump administration of C18 increased body weight relative to vehicle-treated mice, and this effect was primarily associated with a blockade of surgery-induced weight loss on the day after mini-pump implantation (Fig. 5J). Thus, MC3R-specific agonists represent a strategy to promote food intake and weight gain.

Because MC3R KO mice exhibited increased anxiety-like behavior and ARH MC3R neurons bidirectionally regulate anxiety-related behavior, we next tested the effects of acute MC3R stimulation on anxiety. Administration of C18 (5 μg, icv) increased the time spent in the open arms during the EPM test, with similar results observed in both male and female mice (Fig. 5K). No difference in locomotion was detected between vehicle and C18 treatment groups, indicating that the observed effects on anxiety-related behavior were not secondary to changes in locomotion (Fig. 5L). Therefore, MC3R agonists both stimulate feeding and reduce anxiety-related behavior, recapitulating the effects observed after chemogenetic stimulation of ARH MC3R neurons.

MC3R-specific antagonists suppress feeding in mice

Because MC3R stimulation promoted feeding, we next used a recently published MC3R-specific antagonist, referred to here as compound 11 (C11; 5 μg, icv) (20), to test the effect of MC3R inhibition on feeding behavior. C11 administration profoundly suppressed feeding, producing a nearly fourfold decrease in 6-hour food intake relative to vehicle-treated mice

(Fig. 6, A and B, and fig. S11; male mice are shown in Fig. 6 unless otherwise noted) and reduced 24-hour food intake and body weight (Fig. 6, B and C, and fig. S11). Similar results were obtained with female mice (fig. S12). No change in food intake was observed after C11 treatment in MC3R KO mice, indicating that the anorexic effects of C11 were specific to inhibition of MC3R (Fig. 6, D and E).

Because inhibition of MC3R resulted in anorexia and MC3R KO mice exhibit enhanced behavioral anorexia, we tested whether inhibition of MC3R could enhance anorexic responses to pharmacological anorexia. We administered liraglutide, a glucagon-like peptide-1 receptor agonist and obesity therapeutic (34), to WT and MC3R KO (TB/TB) mice (mixed data from male and female mice; fig. S15). No difference in food intake was observed between WT and MC3R KO (TB/TB) mice in response to control saline injections (fig. S15A). However, acute administration of liraglutide produced a greater inhibition of food intake in MC3R KO than WT mice (fig. S15B). The enhanced anorexic response to a single injection of liraglutide lasted for at least 10 days after a single treatment, with daily food intake remaining lower in MC3R KO (TB/TB) mice for 6 days after liraglutide treatment (fig. S15B).

Although both WT and MC3R KO (TB/TB) mice lost weight in response to liraglutide treatment, MC3R KO (TB/TB) mice exhibited a greater and more sustained weight loss and reduction of food intake with repeated doses of liraglutide (fig. S15C). Upon cessation of liraglutide treatment, WT mice returned to their baseline body weight and food intake 24 hours after treatment, whereas MC3R KO (TB/TB) mice maintained a lower body weight for at least 1 week (fig. S15, C and D). These results indicate that genetic deletion of MC3R results in an enhanced anorexic response to pharmacological anorexia, suggesting that MC3R antagonism may both facilitate weight loss and inhibit weight regain.

We next tested whether pharmacological inhibition of MC3R enhanced liraglutide-induced anorexia. Consistent with previous results, liraglutide reduced food intake and body weight (Fig. 6, F and G). Furthermore, coadministration of C11 enhanced the acute anorexic and weight loss effects of liraglutide (Fig. 6, F and G).

We previously observed that MC3R KO mice exhibit a sexually dimorphic anorexia phenotype in the NSF test. To test whether acute pharmacological inhibition of MC3R produced the same anxiogenic and anorexic effects as genetic removal of MC3R, we repeated NSF assays in male and female mice after administration of the MC3R antagonist C11 or vehicle. Acute administration of C11 increased latency to feeding but did not alter total time eating or locomotion (fig. S16). Therefore, MC3R inhibition suppresses feeding without recapitulating the enhanced food avoidance phenotype observed in MC3R KO mice.

In addition to enhanced anorexia, MC3R KO mice displayed an impaired orexigenic response to fasting, gaining less weight than WT mice after refeeding. To test whether pharmacological inhibition of MC3R could also suppress the orexigenic drive associated with hunger, we administered the MC3R antagonist C11 once daily for 3 days after an overnight fast and found that daily administration of C11 reduced body weight gain (Fig.

6H). Together, these findings indicate that MC3R inhibition can enhance anorexic stimuli while also reducing the magnitude of orexigenic stimuli.

AgRP circuitry is required for the feeding effects of MC3R compounds

Although pharmacological stimulation of MC3R and chemogenetic activation of ARH MC3R neurons both robustly stimulated feeding, we sought further data to test the hypothesis that these effects require AgRP neural circuitry. First, we used a chemogenetic inhibition approach to selectively inhibit AgRP neurons before MC3R agonist administration (Fig. 7, A and B; data in Fig. 7 generated using male mice). Consistent with our previous findings, stimulation of MC3R with C18 increased food intake (Fig. 7C). However, prior chemogenetic inhibition of AgRP neurons blocked the ability of C18 to increase food intake, indicating that functional AgRP circuitry is required for the acute orexigenic effects of MC3R stimulation. Chemogenetic inhibition of AgRP neurons did not affect acute baseline feeding in ad libitum–fed mice (Fig. 7C). Thus, the observed effects are unlikely to be secondary to anorexic effects of AgRP neuron inhibition.

To further test the role of MC3R in AgRP neurons in the biological response to MC3R compounds, we created mice in which MC3R is expressed only in AgRP neurons by crossing AgRP-Cre mice with MC3R KO (TB/TB) mice [AgRP-MC3R knockin (KI) mice] (Fig. 7D). FISH analysis confirmed selective restoration of MC3R expression in AgRP neurons, with MC3R expression absent in all other cell types and brain regions examined (Fig. 7D). Administration of the MC3R agonist C18 increased feeding in AgRP-MC3R KI mice (Fig. 7E), whereas administration of the MC3R antagonist C11 suppressed feeding (Fig. 7F). To quantify the relative contribution of AgRP neurons to the effects of MC3R-specific compounds, we compared the relative effects of these compounds in WT and AgRP-MC3R KI mice. Pharmacological stimulation and inhibition of MC3R produced similar increases and decreases, respectively, in food intake in both WT and AgRP-MC3R KI mice (fig. S17). Therefore, the acute feeding effects of MC3R compounds appear to be largely reconstituted by reexpression of the MC3R solely in AgRP neurons.

MC3R stimulation inhibits PVN MC4R neurons in vivo

We previously demonstrated using slice electrophysiology that MC3R regulates presynaptic release of GABA from AgRP neuronal terminals projecting to PVN MC4R neurons (14). On the basis of this finding, and the dependence of MC3R-specific compounds on intact AgRP circuitry (Fig. 7), we hypothesized that pharmacological stimulation of MC3R may engage presynaptic MC3R on AgRP projections in PVN, leading to release of GABA onto PVN MC4R neurons, inhibition of these neurons, and stimulation of food intake. To determine the in vivo effect of MC3R stimulation on PVN MC4R neurons, we targeted viral vectors expressing the genetically encoded calcium indicator GCAMP6s in a Cre-dependent manner to the PVN in MC4R-Cre mice. A gradient refractive index lens was positioned directly above the PVN, which was connected to a miniaturized head-mounted microscope for recording neuronal dynamics in individual PVN MC4R-expressing neurons (Fig. 8, A and B; data in Fig. 8 generated using male mice). Both peripheral administration of the MC3R agonist C18 [Fig. 8C; 10 mg/kg, intraperitoneally (ip)], and intra-PVN administration of C18 (Fig. 8D) increased food intake. No change in calcium signal was detected after a

control saline injection (Fig. 8E and movie S3). Conversely, peripheral administration of an orexigenic dose of the MC3R agonist C18 (Fig. 8C and movie S4) reduced the activity of PVN MC4R neurons (Fig. 8, F and G). In total, about 75 percent of PVN MC4R neurons were inhibited by C18 treatment, whereas 15% increased their activity, and 10% exhibited no change in activity (Fig. 8H). Together, these findings (Figs. 7 and 8) support a model in which MC3R agonists increase food intake by stimulating GABA release from presynaptic AgRP neuronal terminals onto PVN MC4R neurons (fig. S18).

DISCUSSION

The MC3R exhibits dense expression in multiple medial basal hypothalamic structures, including the ARH. The overall distribution of MC3R neurons observed in this study corresponds well with previous descriptions (16). However, the MC3R was originally reported to be expressed in only 50% of orexigenic AgRP neurons (17). In contrast with these findings, we show here that nearly 100% of *Agrp* neurons express *Mc3r* in both male and female mice. This increased detection is likely due to the enhanced sensitivity afforded by RNAscope FISH technology. We also demonstrate that the *Mc3r* exhibits sexually dimorphic expression in multiple hypothalamic nuclei. For example, although the number of *Mc3r*-positive ARH *Agrp* and *Pomc* neurons was similar in female and male mice, there was a large sexual dimorphism in the ARH overall, with more *Mc3r*-positive cells and more *Mc3r* mRNA in males. In contrast, we report a much greater number of *Mc3r* neurons in the AVPV of female versus male mice, demonstrating the complexity of the sexually dimorphic MC3R circuitry.

Although we observed no differences in DREADD-mediated and pharmacologically mediated effects on feeding between male and female mice, we noted profound sexual dimorphisms in MC3R KO mice when we examined the effects of behavioral stressors on food intake. Compared to WT mice, both male and female MC3R KO mice exhibited enhanced anorexia after social isolation, whereas only male MC3R KO mice exhibited enhanced anorexia after restraint. In contrast, female MC3R KO mice exhibited an enhanced anorexic response in the NSF test, although a less pronounced phenotype was also observed in male MC3R KO mice. This assay measures the competition between two motivational states, hunger and the fear and anxiety associated with entrance to the center of an open field. Female MC3R KO mice exhibited a more profound behavioral phenotype in this assay, suggesting that the MC3R KO mouse may model the sexually dimorphic effects of anxiety on feeding in the face of hunger, a model that shares some characteristics with anorexia nervosa, such as food avoidance and elevated anxiety. Further work is clearly necessary to provide a detailed map of the specific neural circuitry contributing to the sex differences observed in stress-induced anorexia in the MC3R KO mouse. Additional studies will also be necessary to fully dissect the relative contribution of anxiety versus defective hunger sensing in the sexually dimorphic behaviors observed in the absence of MC3R. This is of particular importance because human eating disorders exhibit sexual dimorphism, with 90 to 95% of anorexia nervosa cases being observed in females (35, 36), whereas 60% of avoidant-restrictive food intake disorder cases are reported in males (37).

Although MC3R is expressed in multiple cell types in the ARH, data presented here demonstrate that the net effect of activation or inhibition of ARH MC3R neurons on feeding and anxiety resembles AgRP neuronal manipulation in both male and female mice. Consistently, pharmacological manipulation of the MC3R bidirectionally regulated feeding, with MC3R agonists stimulating feeding and MC3R antagonists suppressing feeding. Furthermore, despite the presence of MC3R in POMC neurons and other anorexic neuronal populations such as the paraventricular nucleus of the thalamus (14, 38), ablation of all MC3R-containing cells produced an anorexia and starvation phenotype, clearly demonstrating the dominant effect of MC3R in orexigenic cell types. The findings presented here parallel, across the entire MC3R circuitry, recent data showing the dominance of the orexigenic activity of AgRP neurons over anorexigenic POMC neurons (39). Further anatomical and physiological findings demonstrate that whereas AgRP neurons project to, and directly inhibit, POMC neurons via the release of GABA, POMC neurons do not send projections to the AgRP cell bodies (15, 40–42). Thus, although MC3R is expressed in multiple cell types, and we cannot exclude MC3R-mediated effects via POMC and other ARH MC3R populations for behaviors beyond feeding, the dominant effect of MC3R manipulation on feeding is mediated by AgRP neurons. The MC3R circuitry may be thought of as a bipartite system, with the dominant AgRP MC3R neurons projecting to, and inhibiting, most secondary MC3R neurons [such as POMC neurons (39)] that provide specialized inputs to energy homeostasis, such as the sexually dimorphic circuits characterized here that may communicate information about reproductive state or status to the control of energy homeostasis.

The MC3R is thus a promising pharmacological target for the bidirectional control of energy homeostasis. This potential target may have applications to both obesity and weight loss and to eating disorders such as anorexia nervosa or cachexia, particularly given the ability of MC3R neuron activation and agonist administration to increase feeding and decrease anxiety. Consistent with this notion, MC3R KO mice are hypersensitive to remarkably diverse anorexigenic stimuli including cancer cachexia (43, 44), social isolation, restraint stress, and liraglutide administration. MC3R KO mice also exhibit impaired orexigenic responses to negative energy balance (14), with a marked impairment in refeeding after an overnight fast (14). The enhanced anorexia and impaired orexigenic drive observed in the MC3R KO mouse were not solely produced by developmental effects because pharmacological inhibition of MC3R both enhanced the anorexic response to liraglutide and suppressed the orexigenic response to fasting. Therefore, pharmacological inhibition of MC3R may provide an approach to enhance anorexic responses and also inhibits the normal hunger drive and neuroendocrine responses associated with negative energy balance. This combination of effects may be particularly useful for promoting weight loss in the context of dieting.

The limited chronic drug studies presented here highlight the need for additional work to determine the efficacy of long-term manipulation of the MC3R. Further studies should also address the potential for adverse side effects, such as increased anxiety or aversion, after chronic MC3R inhibition, and should also examine the effects of both MC3R agonists and antagonists on cardiovascular functions, given the well-documented pressor effects of MC4R agonists.

In conclusion, the findings presented here demonstrate that the MC3R is a promising drug target to regulate feeding. With three recent U.S. Federal Drug Administration approvals of melanocortin-based peptide therapeutics (Scenesse, Vyleesi, and Imcivree), it is now clear that melanocortin peptides can make safe and effective drugs (45–50). Further peptide or small-molecule drug development, however, will be needed to test the clinical applications of MC3R modulation described here and to determine whether these compounds can be safely administered in humans. Together, the anatomical, pharmacological, and genetic data presented here support the utility of inhibiting MC3R in both sexes for promoting weight loss; identify MC3R agonism as a potential therapeutic strategy to increase feeding and weight gain while reducing anxiety for the treatment of diverse forms of eating disorders; and identify the MC3R KO mouse as a model for studying sexually dimorphic effects of anxiety on feeding in the face of hunger, as seen in diseases such as anorexia nervosa.

MATERIALS AND METHODS

Study design

In this study, we used neuroanatomical characterization, genetic modeling, DREADD technology, peptide administration, and in vivo endomicroscopy to study the role of MC3R and MC3R-expressing neurons in the regulation of feeding behavior. All experiments were conducted in the inbred C57BL/6J mouse strain because this strain is the most commonly used mouse strain for the study of feeding behavior and energy homeostasis. This animal model appears to be valid for the study of human melanocortin signaling because phenotypes resulting from defects in melanocortin signaling in humans are well replicated in this mouse strain. Animals were randomized in all experiments, and where possible (for example, in pharmacological experiments), experiments were conducted with the investigator blinded regarding the treatment. Data for all graphs are found in data file S2. All experiments were previously approved by the University of Michigan and Vanderbilt University Institutional animal care and use offices (Institutional Animal Care and Use Committee).

Animals

Experiments were performed on adult (8- to 12-week-old) male and female mice. For all feeding and behavioral assays, mice were matched for gender, age, and body weight. Gender differences in behavioral assays are depicted in either the main text or the extended figures. All mice were group-housed on a 12-hour light/12-hour dark cycle and provided ad libitum access to food (5LOD, abDiet) and water before stereotaxic surgeries or behavioral experiments. All mice were group housed for behavioral experiments (OFT, EPM, and NSF tests). For feeding assays, mice were single-housed for at least 2 weeks before starting feeding measurements. Mouse strains used in this study included C57BL/6J (the Jackson laboratory), AgRP-ires-Cre (the Jackson laboratory), MC4R-Cre (the Jackson laboratory), MC3R-KO (bred in-house), MC3R loxTB/TB (the Jackson laboratory), and MC3R-Cre. MC3R-Cre mice were created by the Vanderbilt Transgenic Mouse Resource and were previously described (14). As reported (14), dual RNA FISH was used to validate that Cre-expressing cells also expressed *Mc3r* mRNA in the adult. All mice were bred and

maintained on a C57/BL6J background except for AgRP-ires-Cre mice that were maintained on a mixed background.

Social isolation–induced anorexia

Daily body weight and food intake was recorded from group-housed mice (two to five mice per cage). Food intake was calculated by dividing the daily food intake by the number of mice in each cage. After 2 to 5 days of daily food intake and body weight measurements, all mice were individually housed in the early afternoon (12 p.m.). Acute food intake as well as daily food intake and body weight were recorded at 1, 2, and 4 hours after single housing.

Restraint stress–induced anorexia

Restraint stress–induced anorexia experiments were performed on group-housed mice (two to five mice per cage). Before beginning restraint, daily food intake and body weight was recorded for 5 days (baseline). Food intake was calculated in group-housed mice by averaging the food intake for the cage and dividing by the number of mice in the cage. Food and water were removed from each cage for 30 min daily from 12 p.m. to 12:30 p.m. to account for the time that mice are without food and water during restraint stress. After baseline measurements, mice were restrained daily for 30 min in 50-ml conical tubes from 12 p.m. to 12:30 p.m. Daily food intake and body weight was measured at 12 p.m. After 5 days of restraint, food intake and body weight was measured in the same fashion as the baseline period to test for rebound effects after restraint.

Anxiety behavior assays

Anxiety behavioral assays were performed in the following order with 2 to 4 days separated between each anxiety assay: EPM, OFT, and NSF tests. All behavioral assays were performed during the light cycle between 10 a.m. and 5 p.m. OFT and EPM testing were performed in ad libitum fed–mice with one exception. Chemogenetic inhibition assays (EPM and OFT) were performed on mice fasted overnight (6 p.m. to 10 a.m.) to evaluate inhibition of ARC-MC3R neurons during a time when these cells are expected to be most active (after a fast). For all chemogenetic anxiety assays, CNO was administered 30 min before behavioral testing. For C18 administration, compound was administered 20 min before testing (5 μg, icv).

Open-field test

During testing, mice were placed in the corner of a 50 cm by 50 cm open-field chamber. The center of the arena was marked as the 25 cm by 25 cm area in the center of the open field. Exploratory activity was recorded for 5 min using ANYmaze software (Stoelting). Time in the center, entries to the center, and total distance traveled were automatically recorded with video tracking software. For DREADD-mediated assays, all mice were administered CNO on the day of testing. Differences in open-field activity between DREADD-transduced mice and WT littermates were compared on testing day in response to CNO treatment.

Elevated plus maze

To perform EPM tests, mice were initially placed into the closed arm of the EPM arena. The arena consisted of two 50-cm-long arms. One arm was enclosed by walls, whereas the other arm was open. Activity in the maze was recorded for 5 min using animal tracking software (ANYmaze, Stoelting). Latency to enter the open arms, total distance traveled, entries to open arms, time in open arms, and distance traveled in the open arms were automatically calculated using tracking software. Treatment schedules for the EPM were identical to those described for the OFT.

NSF test

Before testing, mice were fasted overnight (6 p.m. to 10 a.m.). NSF testing was performed in the open-field arena described above. Briefly, a single pellet of palatable high-fat food (3 to 4 g) was placed in the center of the open field. All mice were placed in the corner of the open field, and their activity was automatically scored for 10 min using animal tracking software. Latency to eat the food was manually recorded during testing. Feeding was scored as five consecutive seconds of chewing on the food. Animals were determined to exhibit aphagia if no eating was observed during the 10 min of testing. For pharmacological administration of C11, C11 was administered 20 min before testing (5 μg, icv).

Deletion of MC3R neurons for in vivo study

Heterozygous MC3R-Cre mice (B6.129S4-Mc3rtm1Cone/J; stock no. 007809) were crossed to homozygous R26-LSL-iDTR; (stock no. 007900). The offspring that were positive for one copy of Cre and one DTR gene were selected to study deletion of MC3R-expressing neurons and food intake. MC3R-$Cre^{-/-}$_$DTR^{+/-}$ offspring was used as control. Mice were then singly housed and acclimated to handling and injections. They were then injected twice intraperitoneally with DT (50 μg/kg) or phosphate-buffered saline at days 1 and 3. Food intake and body weight were then monitored for the period of study.

Stereotaxic viral injections and cannula placement

For stereotaxic surgical procedures, mice were anesthetized with isoflurane and placed in a stereotaxic frame (Kopf). A micro-precision drill was used to drill a small burr-hole directly above the viral injection or cannula insertion point, and dura was removed. AAV viral vectors were injected into the ARH using a micromanipulator (Narishige) attached to a pulled glass pipette. For chemogenetic activation experiments, virus was unilaterally injected, whereas bilateral injections were performed for chemogenetic inhibition. Viral injection coordinates for the ARH were as follows: A/P, −1.5 mm (from bregma); M/L, 0.2 mm; and D/V, 5.8 mm (from surface of brain). Viral coordinates for the PVN were as follows: A/P, −0.8 mm (from bregma); M/L, 0.3 mm; and D/V, −4.75 mm (from the surface of the brain). AgRP-Cre mice were injected in the ARH coordinates described above with 250 nl of virus, whereas MC4R-Cre mice were injected into PVN with 500 nl of virus. Virus was injected at a rate of 50 nl/min. After viral injection, the glass pipette was left in place for an additional 5 min to prevent leaking of virus outside the targeted brain region. To target Cre-dependent viral vectors to the ARH of MC3R-Cre mice, 20 nl of virus was injected at a rate of 5 nl/min.

For pharmacological assays, an injection cannula was inserted into the lateral ventricle (LV) or paraventricular hypothalamus. Cannulas were inserted at the following coordinates: A/P, −0.4 mm; M/L, 1.0 mm; and D/V, 2.0 mm (LV) or: A/P, −0.7 mm; M/L, 0.2 mm; and D/V, 4.5 mm (PVN). Cannulas were attached to the skull using Metabond. Two weeks was allotted after surgery to allow for viral expression and the mice to recover from surgical procedures.

Feeding behavior assays

All behavioral assays were performed on ad libitum–fed mice, unless otherwise noted in the main text and figure legends. Mice were single-caged for at least 1 week before starting feeding assays. Feeding assays were performed during the light period.

DREADD feeding assays

To evaluate the effects of DREADD-mediated manipulation of ARH-MC3R neurons on feeding and body weight, we first habituated mice to twice daily vehicle injections (intraperitoneally with saline, 200 μl). After habituation, we administered the DREADD agonist CNO (0.1 mg/kg, 200 μl, ip) twice daily. Injections were performed at 10 a.m. and 6 p.m. Food intake was measured twice daily (10 a.m. and 6 p.m.) during chronic intraperitoneal injection experiments. Body weight was measured daily at 10 a.m. immediately before administering CNO or saline.

MC3R agonist and antagonist feeding assays

For peripheral administration of C18, mice were first habituated to vehicle injections (intraperitoneally with saline, 200 μl) for two to four consecutive days. After habituation and consecutive days of stable food intake in response to saline injections, C18 was administered (10 mg/kg in 200-μl saline, ip). Food intake was measured after drug or vehicle administration by carefully removing food from the food hopper and weighing on a scale. Cages were changed daily during acute feeding assays to prevent spillage of food from the food hopper.

For central administration of MC3R agonist compounds, we first administered vehicle injections [500-nl artificial cerebrospinal fluid (aCSF)] for two to four consecutive days to habituate mice to handling and injection. After consecutive days of stable food intake in response to vehicle, we administered the MC3R agonist C18 (5 μg, 500-nl aCSF). Food intake was measured at ascending time points after vehicle or C18 injections. Central administration of C11 was performed in the same manner as C18 administration except dimethyl sulfoxide (DMSO) was used as vehicle.

For fast-induced feeding assays, mice were fasted overnight (6 p.m. to 12 p.m.) and changed to a fresh cage immediately before fasting. For MC3R KO or WT mice, food was added after an overnight fast, and food intake or body weight was monitored as described above. For pharmacological inhibition of after an overnight fast, C11 was administered (5 μg, icv) 20 min before reintroducing food into the cage, and food intake and body weight were monitored as described above. C11 was administered as previously described on days 2 and 3 and body weight was recording daily immediately before C11 or vehicle administration.

Statistical analysis

After all DREADD viral injections and behavioral experiments, all mice were perfused and location of viral injections or GRIN lens were verified via florescence imaging. Animals with no viral expression or no expression in the ARH were excluded from analysis. Specific statistical analysis is outlined in the figure legends and data file S1. All data were analyzed with GraphPad software. R (v.4.0.0) was used for single-cell RNA sequencing analyses. Data that were normally distributed were analyzed with parametric tests, and data that were not normally distributed were analyzed with nonparametric alternative tests (see the supplementary statistical section for further details). $P \leq 0.05$ was considered significant.

Supplementary Material

Refer to Web version on PubMed Central for supplementary material.

Acknowledgments:

We thank all members of the Cone Lab for comments on early versions of this manuscript, C.-H. Luevano for providing an initial sample of C18, and C. Elias and D. Garcia Galiano for assistance with in situ hybridization. We also thank the Michigan Physiology Phenotyping core for assistance with telemetry experiments and R. Arora for help with illustrations.

Funding:

This work was supported by NIH grants DK070332 and DK126715 (R.D.C.), F32HD095620 (P.S.), K99DK127065 (P.S.), DK106476 (R.B.S.), and F32DK123879 (M.N.B.). The GTEx Project was supported by the Common Fund of the Office of the Director of the NIH and by NCI, NHGRI, NHLBI, NIDA, NIMH, and NINDS.

Data and materials availability:

All data related to the current study are present in the paper or Supplementary Materials. Any materials available may be requested from R.B.S. (in situ hybridization) or R.D.C. (animal strains and pharmacological reagents).

REFERENCES AND NOTES

1. Cone RD, Anatomy and regulation of the central melanocortin system. Nat. Neurosci. 8, 571–578 (2005). [PubMed: 15856065]
2. Sohn JW, Elmquist JK, Williams KW, Neuronal circuits that regulate feeding behavior and metabolism. Trends Neurosci. 36, 504–512 (2013). [PubMed: 23790727]
3. Friedman J, 20 years of leptin: Leptin at 20: An overview. J. Endocrinol. 223, T1–T8 (2014). [PubMed: 25121999]
4. Xu J, Bartolome CL, Low CS, Yi X, Chien CH, Wang P, Kong D, Genetic identification of leptin neural circuits in energy and glucose homeostases. Nature 556, 505–509 (2018). [PubMed: 29670283]
5. Takahashi KA, Cone RD, Fasting induces a large, eptin-dependent increase in the intrinsic action potential frequency of orexigenic arcuate nucleus neuropeptide Y/ Agouti-related protein neurons. Endocrinology 146, 1043–1047 (2005). [PubMed: 15591135]
6. Atasoy D, Nicholas Betley J, Su HH, Sternson SM, Deconstruction of a neural circuit for hunger. Nature 488, 172–177 (2012). [PubMed: 22801496]
7. Li C, Hou Y, Zhang J, Sui G, Du X, Licinio J, Wong ML, Yang Y, AGRP neurons modulate fasting-induced anxiolytic effects. Transl. Psychiatry 9, 111 (2019). [PubMed: 30850579]

8. Burnett CJ, Li C, Webber E, Tsaousidou E, Xue SY, Brüning JC, Krashes MJ, Hunger-driven motivational state competition. Neuron 92, 187–201 (2016). [PubMed: 27693254]
9. Padilla SL, Qiu J, Soden ME, Sanz E, Nestor CC, Barker FD, Quintana A, Zweifel LS, Rønnekleiv OK, Kelly MJ, Palmiter RD, Agouti-related peptide neural circuits mediate adaptive behaviors in the starved state. Nat. Neurosci. 19, 734–741 (2016). [PubMed: 27019015]
10. Campos CA, Bowen AJ, Roman CW, Palmiter RD, Encoding of danger by parabrachial CGRP neurons. Nature 555, 617–622 (2018). [PubMed: 29562230]
11. Luquet S, Perez FA, Hnasko TS, Palmiter RD, NPY/AgRP neurons are essential for feeding in adult mice but can be ablated in neonates. Science 310, 683–685 (2005). [PubMed: 16254186]
12. Aponte Y, Atasoy D, Sternson SM, AGRP neurons are sufficient to orchestrate feeding behavior rapidly and without training. Nat. Neurosci. 14, 351–355 (2011). [PubMed: 21209617]
13. Krashes MJ, Koda S, Ye CP, Rogan SC, Adams AC, Cusher DS, Maratos-Flier E, Roth BL, Lowell BB, Rapid, reversible activation of AgRP neurons drives feeding behavior in mice. J. Clin. Invest. 121, 1424–1428 (2011). [PubMed: 21364278]
14. Ghamari-Langroudi M, Cakir I, Lippert RN, Sweeney P, Litt MJ, Ellacott KLJ, Cone RD, Regulation of energy rheostasis by the melanocortin-3 receptor. Sci. Adv. 4, eaat0866 (2018). [PubMed: 30140740]
15. Cowley MA, Smart JL, Rubinstein M, Cerdán MG, Diano S, Horvath TL, Cone RD, Low MJ, Leptin activates anorexigenic POMC neurons through a neural network in the arcuate nucleus. Nature 411, 480–484 (2001). [PubMed: 11373681]
16. Roselli-Rehfuss L, Mountjoy KG, Robbins LS, Mortrud MT, Low MJ, Tatro JB, Entwistle ML, Simerly RB, Cone RD, Identification of a receptor for gamma melanotropin and other proopiomelanocortin peptides in the hypothalamus and limbic system. Proc. Natl. Acad. Sci. U.S.A. 90, 8856–8860 (1993). [PubMed: 8415620]
17. Bagnol D, Lu XY, Kaelin CB, Day HE, Ollmann M, Gantz I, Akil H, Barsh GS, Watson SJ, Anatomy of an endogenous antagonist: Relationship between Agouti-related protein and proopiomelanocortin in brain. J. Neurosci. 19, RC26 (1999). [PubMed: 10479719]
18. Marks DL, Hruby V, Brookhart G, Cone RD, The regulation of food intake by selective stimulation of the type 3 melanocortin receptor (MC3R). Peptides 27, 259–264 (2006). [PubMed: 16274853]
19. Doering SR, Freeman KT, Schnell SM, Haslach EM, Dirain M, Debevec G, Geer P, Santos RG, Giulianotti MA, Pinilla C, Appel JR, Speth RC, Houghten RA, Haskell-Luevano C, Discovery of mixed pharmacology melanocortin-3 agonists and melanocortin-4 receptor tetrapeptide antagonist compounds (TACOs) based on the sequence Ac-Xaa1-Arg-(pI)DPhe-Xaa4-NH2. J. Med. Chem. 60, 4342–4357 (2017). [PubMed: 28453292]
20. Singh A, Dirain M, Witek R, Rocca JR, Edison AS, Haskell-Luevano C, Structure-activity relationships of peptides incorporating a bioactive reverse-turn heterocycle at the melanocortin receptors: Identification of a 5800-fold mouse melanocortin-3 receptor (mMC3R) selective antagonist/partial agonist versus the mouse melanocortin-4 receptor (mMC4R). J. Med. Chem. 56, 2747–2763 (2013). [PubMed: 23432160]
21. Lippert RN, Ellacott KLJ, Cone RD, Gender-specific roles for the melanocortin-3 receptor in the regulation of the mesolimbic dopamine system in mice. Endocrinology 155, 1718–1727 (2014). [PubMed: 24605830]
22. Kaufmann AS, Coming of age in the kisspeptin era: Sex differences, development, and puberty. Mol. Cell. Endocrinol. 324, 51–63 (2010). [PubMed: 20083160]
23. Campbell JN, Macosko EZ, Fenselau H, Pers TH, Lyubetskaya A, Tenen D, Goldman M, Verstegen AMJ, Resch JM, McCarroll SA, Rosen ED, Lowell BB, Tsai LT, A molecular census of arcuate hypothalamus and median eminence cell types. Nat. Neurosci. 20, 484–496 (2017). [PubMed: 28166221]
24. Zhu C, Jiang Z, Xu Y, Cai Z-L, Jiang Q, Xu Y, Xue M, Arenkiel BR, Wu Q, Shu G, Tong Q, Profound and redundant functions of arcuate neurons in obesity development. Nat. Metab. 2, 763–774 (2020). [PubMed: 32719538]
25. Zhang X, van den Pol AN, Hypothalamic arcuate nucleus tyrosine hydroxylase neurons play orexigenic role in energy homeostasis. Nat. Neurosci. 19, 1341–1347 (2016). [PubMed: 27548245]

26. Jais A, Paeger L, Sotelo-Hitschfeld T, Bremser S, Prinzensteiner M, Klemm P, Mykytiuk V, Widdershooven PJM, Vesting AJ, Grzelka K, Minère M, Cremer AL, Xu J, Korotkova T, Lowell BB, Zeilhofer HU, ackes H, Fenselau H, Wunderlich FT, Kloppenburg P, Brüning JC?, PNOC^{ARC} neurons promote hyperphagia and obesity upon high fat-diet feeding. Neuron 106, 1009–1025 (2020). [PubMed: 32302532]
27. Fenselau H, Campbell JN, Verstegen AMJ, Madara JC, Xu J, Shah BP, Resch JM, Yang Z, Mandelblat-Cerf Y, Livneh Y, Lowell BB, A rapidly-acting glutamatergic ARC→PVN sateity circuit postsynaptically regulated by α-MSH. Nat. Neurosci. 20, 42–51 (2017). [PubMed: 27869800]
28. Bulik CM, Sullivan PF, Tozzi F, Furberg H, Lichtenstein P, Pedersen NL, Prevalence, heritability, and prospective risk factors for anorexia nervosa. Arch. Gen. Psychiatry 63, 305–312 (2006). [PubMed: 16520436]
29. Lee M, Kim A, Conwell IM, Hruby V, Mayorov A, Cai M, Wardlaw SL, Effects of selective modulation of the central melanocortin-3-receptor on food intake and hypothalamic POMC expression. Peptides 29, 440–447 (2008). [PubMed: 18155809]
30. Roth BL, DREADDs for neuroscientists. Neuron 89, 683–694 (2016). [PubMed: 26889809]
31. Padilla SL, Qiu J, Nestor CC, Zhang C, Smith AW, Whiddon BB, Rønnekleiv OK, Kelly MJ, Palmiter RD, AgRP to Kiss1 neuron signaling links nutritional state and fertility. Proc. Natl. Acad. Sci. U.S.A. 114, 2413–2418 (2017). [PubMed: 28196880]
32. Dietrich MO, Zimmer MR, Bober J, Horvath TL, Hypothalamic Agrp neurons drive stereotypic behaviors beyond feeding. Cell 169, 1222–1232 (2015).
33. Klawonn AM, Fritz M, Nilsson A, Bonaventura J, Shionoya K, Mirrasekhian E, Karlsson U, Jaarola M, Granseth B, Blomqvist A, Michaelides M, Engblom D, Motivational valence is determined by striatal melanocortin 4 receptors. J. Clin. Invest. 128, 3160–3170 (2018). [PubMed: 29911992]
34. Nuffer WA, Trujillo JM, Liraglutide: A new option for the treatment of obesity. Pharmacotherapy 35, 926–934 (2015). [PubMed: 26497479]
35. Keski-Rahkonen A, Hoek HW, Susser ES, Linna MS, Sihvola E, Raevuori A, Bulik CM, Kaprio J, Rissanen A, Epidemiology and course of anorexia nervosa in the community. Am. J. Psychiatry 164, 1259–1265 (2007). [PubMed: 17671290]
36. Herpertz-dahlmann B, Holtkamp K, Konrad K, Eating disorders: Anorexia and bulimia nervosa. Handb. Clin. Neurol. 106, 447–462 (2012). [PubMed: 22608637]
37. Zimmerman J, Fisher M, Avoidant/restrictive food intake disorder (ARFID). Curr. Probl. Pediatr. Adolesc. Health Care 47, 95–103 (2017). [PubMed: 28532967]
38. Atasoy D, Sternson SM, Neuroendocrinology of Appetite (John Wiley & Sons, 2016).
39. Wei Q, Krolewski DM, Moore S, Kumar V, Li F, Martin B, Tomerb R, Murphy GG, Deisseroth K, Watson SJ, Akil H, Uneven balance of power between hypothalamic peptidergic neurons in the control of feeding. Proc. Natl. Acad. Sci. U.S.A. 115, E9489–E9498 (2018). [PubMed: 30224492]
40. Mercer AJ, Hentges ST, Meshul CK, Low MJ, Unraveling the central proopiomelanocortin neural circuits. Front. Neurosci. 7, 19 (2013). [PubMed: 23440036]
41. Rau AR, Hentges ST, The relevance of AgRP neuron-derived GABA inputs to POMC neurons differs for spontaneous and evoked release. J. Neurosci. 37, 7362–7372 (2017). [PubMed: 28667175]
42. Hentges ST, Nishiyama M, Overstreet LS, Stenzel-Poore M, Williams JT, Low MJ, GABA release from proopiomelanocortin neurons. J. Neurosci. 24, 1578–1583 (2004). [PubMed: 14973227]
43. Marks DL, Cone RD, The role of the melanocortin-3 receptor in cachexia. Ann. N. Y. Acad. Sci. 1, 258–266 (2003).
44. Marks DL, Butler AA, Turner R, Brookhart G, Cone RD, Differential role of melanocortin receptor subtypes in cachexia. Endocrinology 4, 1513–1523 (2003).
45. Kühnen P, Clément K, Wiegand S, Blankenstein O, Gottesdiener K, Martini LL, Mai K, Blume-Peytavi U, Grüters A, Krude H, Proopiomelanocortin deficiency treated with a melanocortin-4 receptor agonist. N. Engl. J. Med. 375, 240–246 (2016). [PubMed: 27468060]
46. Clément K, Biebermann H, Farooqi IS, Van Der Ploeg L, Wolters B, Poitou C, Puder L, Fiedorek F, Gottesdiener K, Kleinau G, Heyder N, Scheerer P, Blume-Peytavi U, Jahnke I, Sharma S,

Mokrosinski J, Wiegand S, Müller A, Weiß K, Mai K, Spranger J, Grüters A, Blankenstein O, Krude H, Kühnen P, MC4R agonism promotes durable weight loss in patients with leptin receptor deficiency. Nat. Med. 24, 551–555 (2018). [PubMed: 29736023]

47. NCT03746522, Setmelanotide (RM-493), Melanocortin-4 Receptor (MC4R) Agonist, in Bardet-Biedl Syndrome (BBS) and Alström Syndrome (AS) Patients With Moderate to Severe Obesity (2018); http://clinicaltrials.gov/show/nct03746522.
48. Dhillon S, Keam SJ, Bremelanotide: First approval. Drugs 79, 1599–1606 (2019). [PubMed: 31429064]
49. Mayer D, Lynch SE, Bremelanotide: New drug approved for treating hypoactive sexual desire disorder. Ann. Pharmacother. 54, 684–690 (2019).
50. Langendonk JG, Balwani M, Anderson KE, Bonkovsky HL, Anstey AV, Bissell DM, Bloomer J, Edwards C, Neumann NJ, Parker C, Phillips JD, Lim HW, Hamzavi I, Deybach J-C, Kauppinen R, Rhodes LE, Frank J, Murphy GM, Karstens FPJ, Sijbrands EJG, de Rooij FWM, Lebwohl M, Naik H, Goding CR, Wilson JHP, Desnick RJ, Afamelanotide for erythropoietic protoporphyria. N. Engl. J. Med. 373, 48–59 (2015). [PubMed: 26132941]
51. Butler A, Hoffman P, Smibert P, Papalexi E, Satija R, Integrating single-cell transcriptomic data across different conditions, technologies, and species. Nat. Biotechnol. 36, 411–420 (2018). [PubMed: 29608179]
52. Stuart T, Butler A, Hoffman P, Hafemeister C, Papalexi E, Mauck III WM, Hao Y, Stoeckius M, Smibert P, Satija R, Comprehensive integration of single-cell data. Cell 177, 1888–1902 (2019). [PubMed: 31178118]

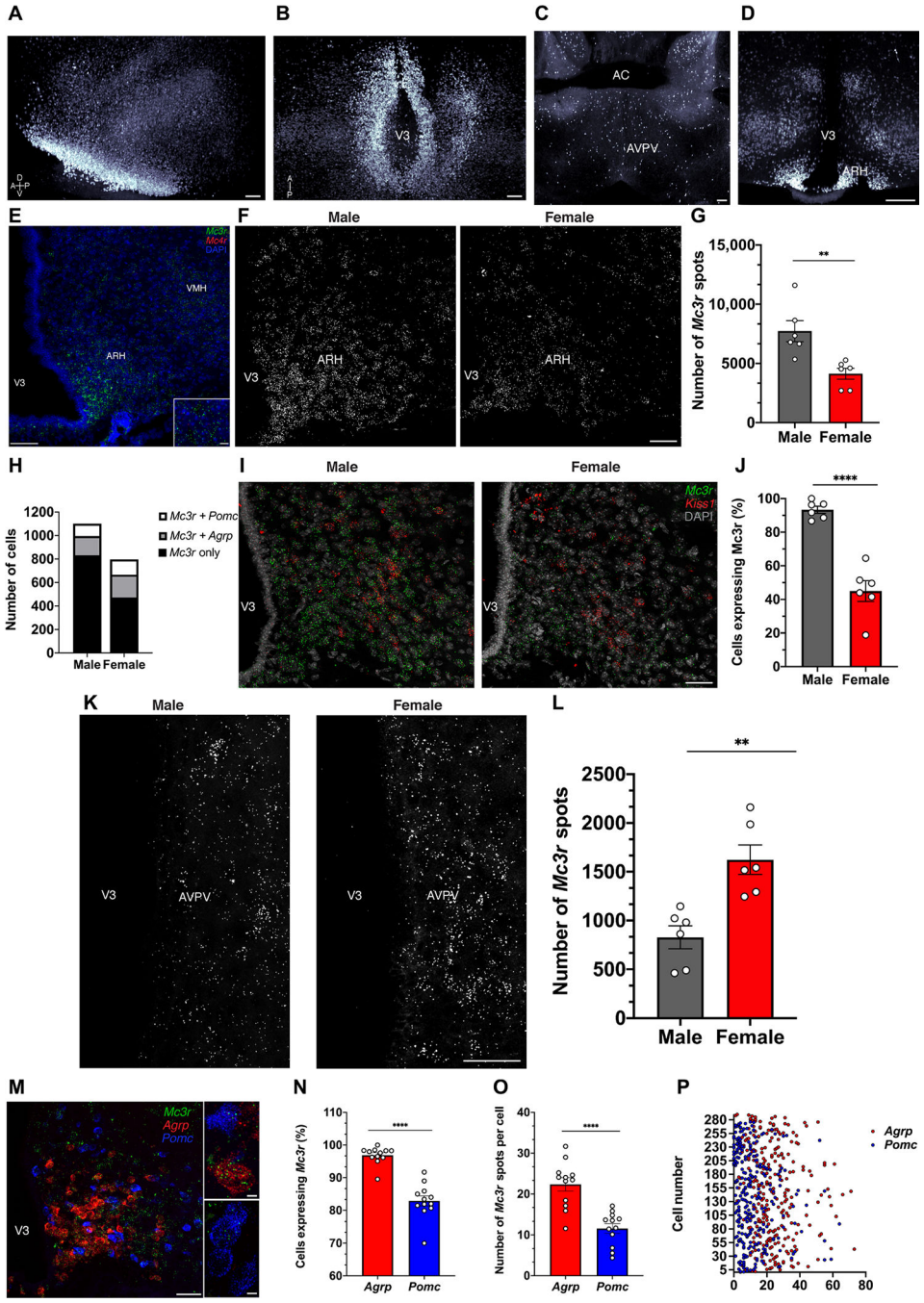

Fig. 1. MC3R expression is abundant and sexually dimorphic in the mouse AVPV and ARH.

(**A**) Three-dimensional rendering of the hypothalamus of a male MC3R-Cre-Rosa26-tdTomato brain viewed in the sagittal plane. Scale bar, 100 μm. (**B**) Ventral view of MC3R-positive neurons in the mediobasal hypothalamus. Scale bar, 100 μm (V3; third ventricle). (**C**) Coronal view of MC3R labeling in the AVPV [anterior-posterior (AP) = 0.26 mm]. Scale bar, 200 μm. AC, anterior commisure. (**D**) Coronal view of MC3R labeling in the ARH (AP = −1.70 mm). Scale bar, 200 μm. (**E**) Low-magnification image of *Mc3r* mRNA (green), *Mc4r* mRNA (red), and 4',6-diamidino-2-phenylindole (DAPI) (blue) in

the ARH and ventromedial hypothalamus (VMH) (AP = −1.82 mm). Scale bar, 100 μm. High-magnification inset illustrates *Mc3r* and *Mc4r* expression in ARH neurons. Scale bar, 10 μm. (**F**) RNAscope analysis of *Mc3r* mRNA expression in the ARH in male (left) and female mice (middle) (AP = −1.70 mm). Scale bar, 50 μm. (**G**) *Mc3r* mRNA abundance (n = 6 male and 6 female mice). Student's unpaired t test, $^{**}P < 0.01$. (**H**) Distribution of *Mc3r*-positive cells containing *Pomc*, *Agrp*, or only *Mc3r*. (**I**) RNAscope analysis of *Mc3r* (green) expression in *Kiss1* neurons (red) in the ARH in male (left) and female mice (right) (AP = −1.58 mm). Scale bar, 50 μm. (**J**) Percentage of *Kiss1* neurons expressing *Mc3r* in the ARH (n = 6 male and 6 female mice). Student's unpaired t test, $^{****}P < 0.001$. (**K**) RNAscope analysis of *Mc3r* mRNA expression in the anteroventral periventricular area in male (left) and female mice (middle) (AP = 0.26 mm). Scale bar, 50 μm. (**L**) *Mc3r* mRNA as abundance (n = 6 male and n = 6 female mice). Student's unpaired t test, $^{**}P < 0.01$. (**M**) Low-magnification image of *Mc3r* (green), *Agrp* (red), and *Pomc* (blue) mRNA labeling in the ARH (left) (AP = −1.70 mm). Scale bar, 50 μm. Right: High-magnification images illustrating *Mc3r* expression in *Agrp* and *Pomc* neurons. Scale bars, 5 μm. (**N**) Percentage of *Agrp* and *Pomc* neurons expressing *Mc3r* in the ARH (n = 6 male and n = 6 female). Data analyzed with Student's unpaired T test. $^{****}P < 0.001$. (**O**) Number of *Mc3r* spots per cell in *Agrp* and *Pomc* neurons in the ARH (n = 6 male and 6 female mice). Data analyzed with Student's unpaired T test. $^{****}P < 0.001$. (**P**) Distribution of the number of *Mc3r* spots for each *Agrp* and *Pomc* neuron analyzed.

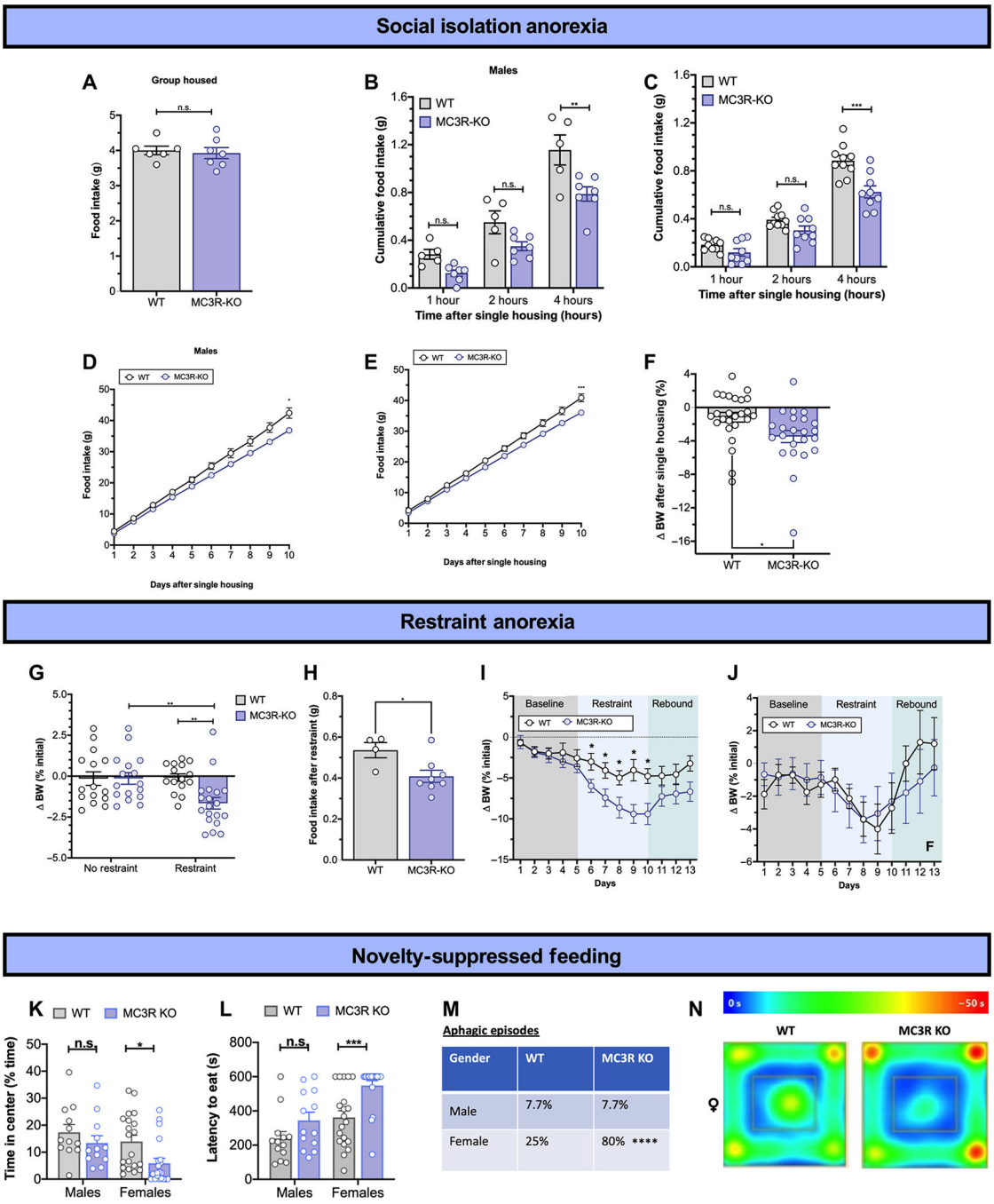

Fig. 2. Sexually dimorphic anorexia in the MC3R KO mouse.

(**A**) Body weight (BW) of WT and MC3R KO mice used in social isolation–induced anorexia experiments ($n = 7$ cages per group; 4 males and 3 females). (**B** and **C**) Food intake in male and female WT and MC3R KO mice after single housing [$n = 5$ mice for WT group and $n = 7$ MC3R KO mice in (B), $n = 10$ WT mice and $n = 9$ MC3R KO mice in (C)]. (**D** and **E**) Cumulative food intake in male and female WT and MC3R KO mice after social isolation [$n = 5$ mice for WT group and $n = 7$ MC3R KO mice in (D), $n = 10$ WT mice and $n = 9$ MC3R KO mice in (E)]. (**F**) Change in body weight in male and female WT and

MC3R KO mice after social isolation (n = 12 WT male and 13 WT female mice, and n = 12 male MC3R KO and 11 female MC3R KO mice). (**G**) Change in body weight 24 hours after restraint stress (n = 15 male mice for no restraint WT group, n = 16 male mice for no restraint MC3R KO group, n = 15 male mice for restraint WT group, n = 19 male mice for restraint MC3R KO group). (**H**) Food intake in male WT and MC3R KO mice after restraint stress. Data points represent individual cages. Food intake was calculated by dividing food intake for the cage by the number of mice in the cage (n = 8 cages for MC3R KO group and n = 4 cages for WT group). (**I** and **J**) Change in body weight during chronic daily restraint stress in WT and MC3R KO males (I) and females (J) [n = 8 WT mice and n = 9 MC3R KO mice in (I), n = 7 WT mice and n = 11 MC3R KO mice in (J)]. (**K** and **L**) Time in center (K) and latency to eat (L) during novelty-suppressed feeding (NSF) tests. (**M**) Chart showing percentage of mice in each group that did not eat during testing (aphagic episodes) [n = 13 male WT mice, n = 20 female WT mice, n = 13 MC3R KO males, and n = 20 MC3R KO females for (K) to (M)]. (**N**) Heat plot showing amount of time spent in each area of the open field for WT and MC3R KO mice during NSF testing. Data are represented as means ± SEM. (A), (F), and (H) analyzed by unpaired Student's t test; (C) to (E), (G), and (I) to (L), by two-way analysis of variance (ANOVA) with Sidak's post hoc test. *P < 0.05, **P < 0.01, ***P < 0.005, and ****P < 0.001. n.s., not significant.

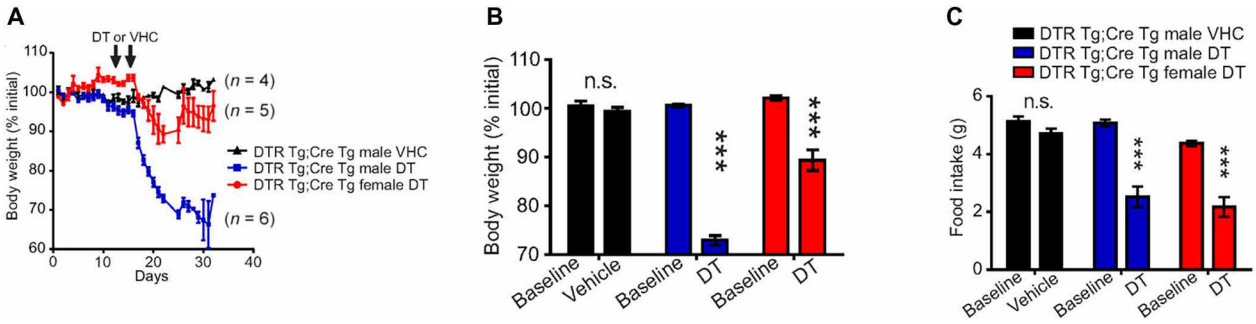

Fig. 3. Ablation of MC3R neurons leads to anorexia and starvation.

(**A**) Change in body weight after diphtheria toxin (DT)– mediated ablation of MC3R neurons. (**B**) Change in body weight after DT injections in combined male and female MC3R-Cre mice ($n = 5$ DT females, $n = 6$ DT males, and $n = 4$ WT males). (**C**) Daily food intake after DT or vehicle (VHC) injection to male MC3R-Cre DTR transgene and female MC3R-Cre DTR transgenic mice. Data presented as means ± SEM ANOVA, ***$P < 0.001$.

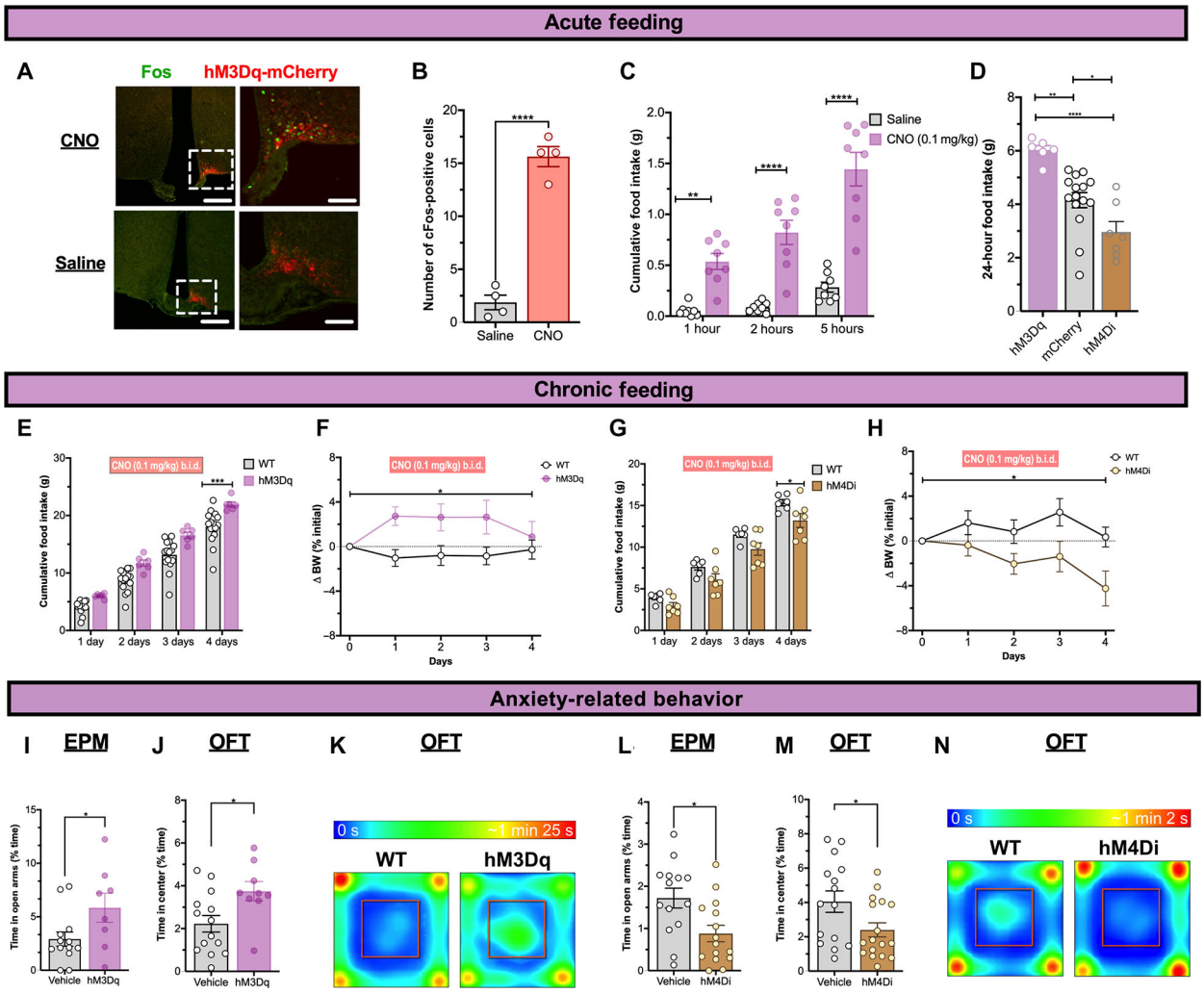

Fig. 4. ARH MC3R neuron activation increases feeding and reduce anxiety.

(**A**) Representative image showing expression of hM3Dq-mCherry and cFos in the ARH of an MC3R-Cre mouse after intraperitoneal injections of CNO or saline. Scale bar, 500 μm. Zoomed-in images of hM3Dq-mCherry and cFos expression are shown in the right column. Scale bar, 50 μm. (**B**) Quantification of the number of cFos-positive cells in response to CNO injection ($n = 4$ per group). (**C**) Cumulative food intake after a single CNO (0.1 mg/kg) or saline injection in mice transfected with hM3Dq-mCherry in ARH MC3R neurons ($n = 8$ male mice in saline and CNO groups). (**D**) Twenty-four–hour food intake after CNO injection in mice expressing hM3Dq, hM4Di, or control mCherry in ARH MC3R neurons ($n = 6$ male mice in hM3Dq group, $n = 15$ male mice in mCherry group, and $n = 7$ male mice in hM4Di group). (**E**) Cumulative food intake in response to CNO in MC3R-Cre mice transfected with hM3Dq-mCherry in ARH or littermate control mice ($n = 6$ male mice for hM3Dq group and $n = 15$ male mice for WT group). b.i.d. (twice daily). (**F**) Change in body weight after twice daily administration of CNO to hM3Dq-mCherry–transduced or littermate control mice ($n = 6$ male mice for hM3Dq group and $n = 15$ male mice for WT group). (**G**) Cumulative food intake after twice daily CNO administration to mice transduced with hM4Di-mCherry in ARH-MC3R neurons or WT control littermate mice ($n = 6$ male

mice for WT group and $n = 7$ male mice for hM4Di group). (**H**) Change in body weight after twice daily administration of CNO ($n = 6$ male mice for WT group and $n = 7$ male mice for hM4Di group). (**I** and **J**) Time in the open arms (I) and in the center of the open field (J) during behavioral testing ($n = 11$ male mice for WT group and $n = 11$ male mice for hM3Dq group). (**K**) Heat plot showing average amount of time spent in each area of the open field for WT and hM3Dq-transduced mice. Data shown from time 0 to 1 min 25 s. (**L** and **M**) Time in the open arms (L) and in the center (M) during EPM and OFT in mice targeted with hM4Di in ARH-MC3R neurons ($n = 14$ male mice for WT group and $n = 15$ male mice for hM4Di group). (**N**) Heat plot showing average amount of time spent in each area of the open field for WT and hM4Di-transduced mice. Data shown from time 0 to 1 min 2 s. Data shown as means ± SEM CNO (0.1 mg/kg, ip) was administered 30 min before behavioral testing in all mice. Data show combined male and female mice. Similar results were obtained in both male and female mice (see fig. S8). Data analyzed with Student's unpaired *t* test (B, I, J, L, and M), two-way ANOVA with Sidak's post hoc test (C, E, F, G, and H), or one-way ANOVA (D). $*P < 0.05$, $**P < 0.01$, $***P < 0.005$, and $****P < 0.001$.

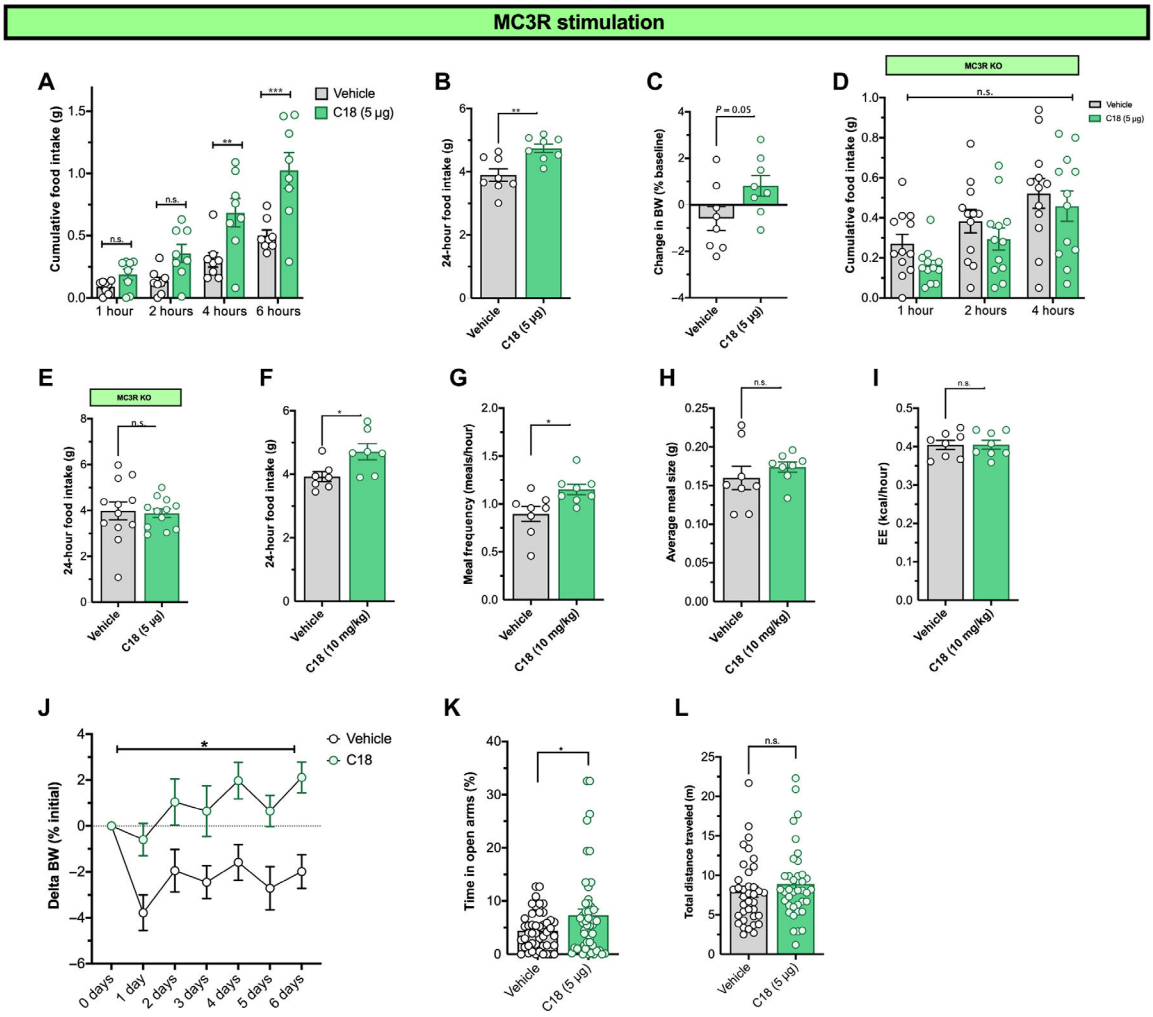

Fig. 5. MC3R stimulation increases feeding.

(**A**) Cumulative food intake in WT mice after administration of vehicle (aCSF) or the MC3R agonist C18 (5 µg, icv). (**B**) 24-hour food intake after administration of vehicle (aCSF) or C18 to WT mice. (**C**) Change in body weight after injection of vehicle or C18 (5 µg) [$n = 7$ male mice and $n = 8$ male mice for vehicle and C18 groups in (A) to (C)]. (**D** and **E**) Cumulative food intake (D) and 24-hour food intake (E) after C18 or vehicle administration in MC3R KO mice [$n = 12$ male mice for vehicle and C18 group in (D) and (E)]. (**F** to **H**) Twenty-four–hour food intake (F), meal frequency (G), and average meal size (H) after vehicle or C18 administration (10 mg/kg, ip) in CLAMS metabolic cages. (**I**) Energy expenditure after administration of vehicle or C18 in metabolic cages [$n = 8$ male mice for vehicle and C18 group in (F) to (I)]. (**J**) Change in body weight after mini-pump implantation of either vehicle or C18 (10 mg/kg per day for 6 days) ($n = 5$ mice for C18 group and $n = 5$ mice for vehicle group). (**K** and **L**) Time in the open arms (K, percent time in open arms) and total distance traveled (L) EPM testing [$n = 46$ male mice for vehicle group and $n = 50$ male mice for C18 group in (K), $n = 37$ male mice for vehicle group, and $n = 38$ male mice for C18 group in (L)]. Data presented as means ± SEM. (A), (D), and (J) analyzed by repeated measures two-way ANOVA with Sidak's post hoc test. (B), (C), (E),

(F), (G), (H), (I), (K), and (L) analyzed with unpaired Student's *t* test. *$P < 0.05$, **$P < 0.01$, ****$P < 0.001$.

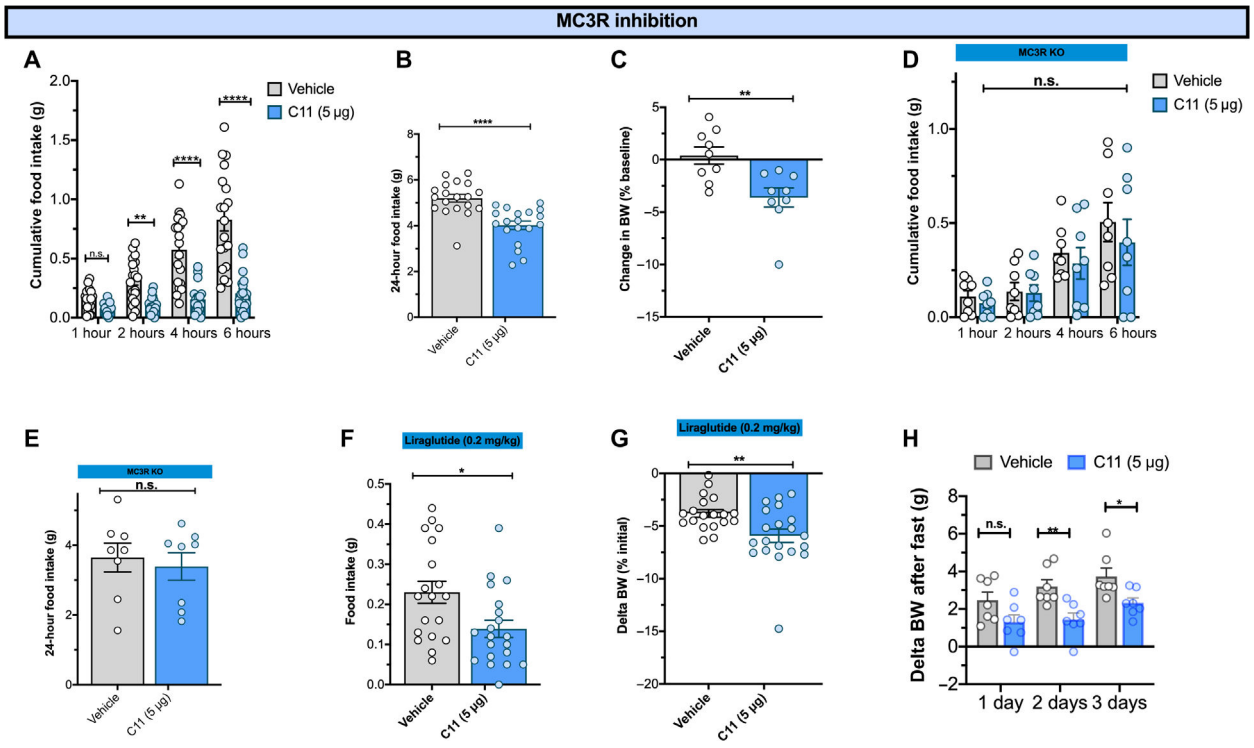

Fig. 6. Pharmacological inhibition of MC3R suppresses feeding in mice.

(**A**) Cumulative food intake after administration of the MC3R antagonist compound 11 (C11) or vehicle. (**B**) Twenty-four–hour food intake after administration of vehicle or C11 (5 μg) [n = 19 male mice for both vehicle and C11 groups in (A) and (B)]. (**C**) Change in body weight after injection of vehicle or C11 (5 μg) (n = 9 male mice for vehicle and C11 groups). (**D** and **E**) Food intake after intracerebroventricular injection of vehicle (DMSO, 500 nl) or C11 (5 μg, 500 nl) in MC3R KO mice [n = 8 male mice for both vehicle and C11 groups in (D) and (E)]. (**F**) Food intake after acute liraglutide administration [0.2 mg/kg, subcutaneously (sc)] during coadministration of vehicle (500-nl DMSO, icv), or C11 (500 nl in DMSO, icv). (**G**) 24-hour change in body weight after acute coadministration of either liraglutide (0.2 mg/kg, sc) and vehicle (intracerebroventricular DMSO, 500 nl), or liraglutide (0.2 mg/kg, sc) and MC3R antagonist C11 (5 μg, icv) [n = 19 male mice for both vehicle and C11 group in (F) and (G)]. (**H**) Change in body weight after refeeding from an overnight fast. C11 or vehicle was administered daily immediately before refeeding (n = 7 male mice for both the vehicle and C11 groups). Data presented as means ± SEM. Data in (A), (D), and (H) were analyzed with repeated measures two-way ANOVA and Sidak's post hoc test. Data in (B), (C), (E) (F), and (G) were analyzed with unpaired Student's t test. *P < 0.05, **P < 0.01, and ****P < 0.001.

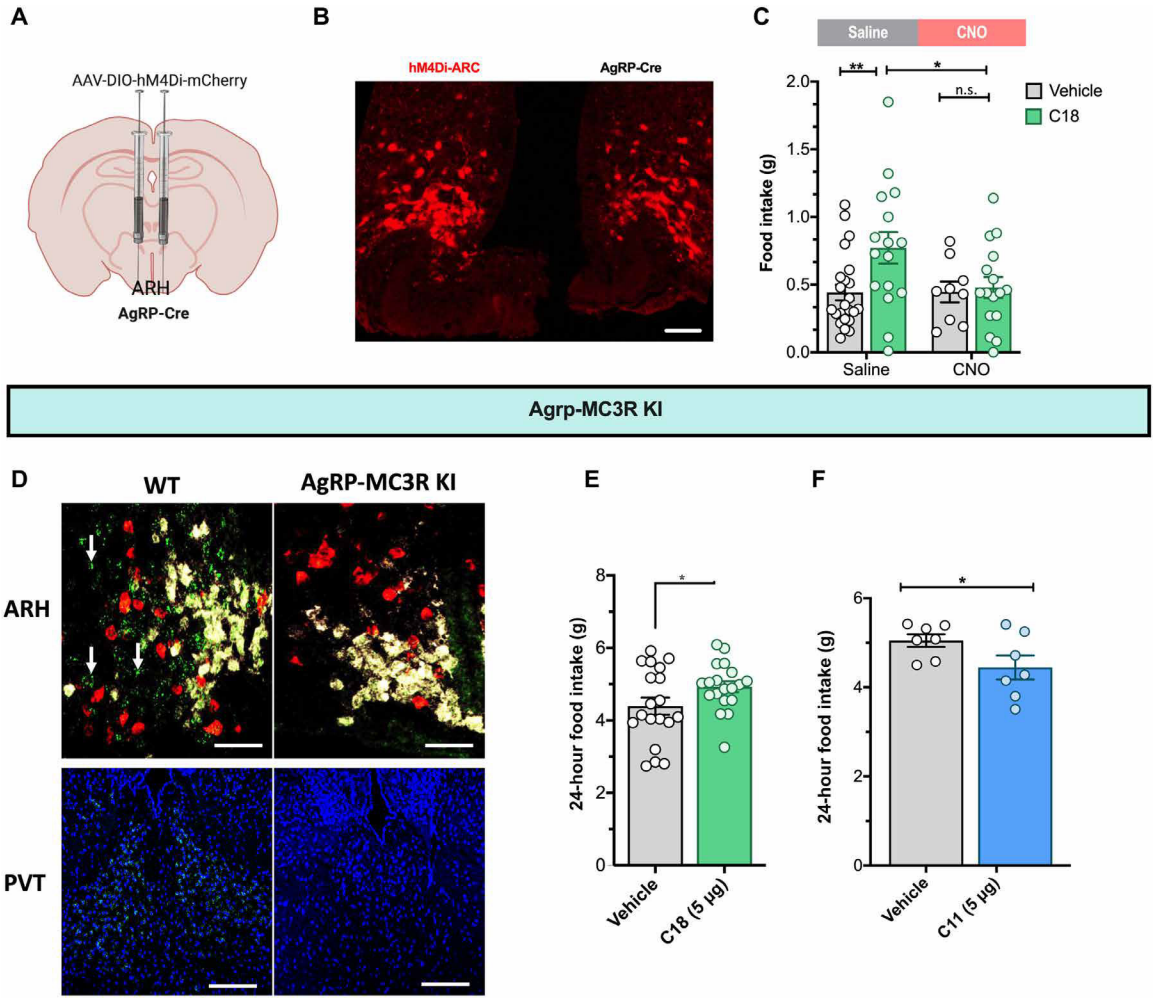

Fig. 7. MC3R-specific compounds regulate feeding via AgRP circuitry.

(**A** and **B**) Schematic of experimental strategy to express inhibitory DREADD virus in hypothalamic AgRP neurons (A) and representative image of DREADD-transduced AgRP neurons (B). Scale bar, 200 µm. (**C**) Food intake after administration of C18 in the presence of saline or CNO (0.1 mg/kg, ip) (n = 20 male mice for vehicle saline group, n = 12 male mice for vehicle C18 group, n = 9 male mice for CNO vehicle group, and n = 15 male mice for CNO C18 group). (**D**) RNAscope analysis of MC3R expression in WT and AgRP-MC3R KI mice. Scale bar, 500 µm. PVT, paraventricular nucleus of the thalamus. (**E**) Food intake 24 hours after administration of vehicle or C18 to AgRP-MC3R KI mice (n = 19 male mice for vehicle and C18 groups). (**F**) Food intake 24 hours after administration of vehicle of C11 to AgRP-MC3R KI mice (n = 7 male mice for vehicle and C11 groups). Feeding experiments performed in the early afternoon (12 p.m.) and food intake in (C) represent food intake 4 hours after injections. (C) analyzed by two-way ANOVA with Sidak's post hoc test. (E) and (F) analyzed by Student's t test. *P < 0.05, **P < 0.01.

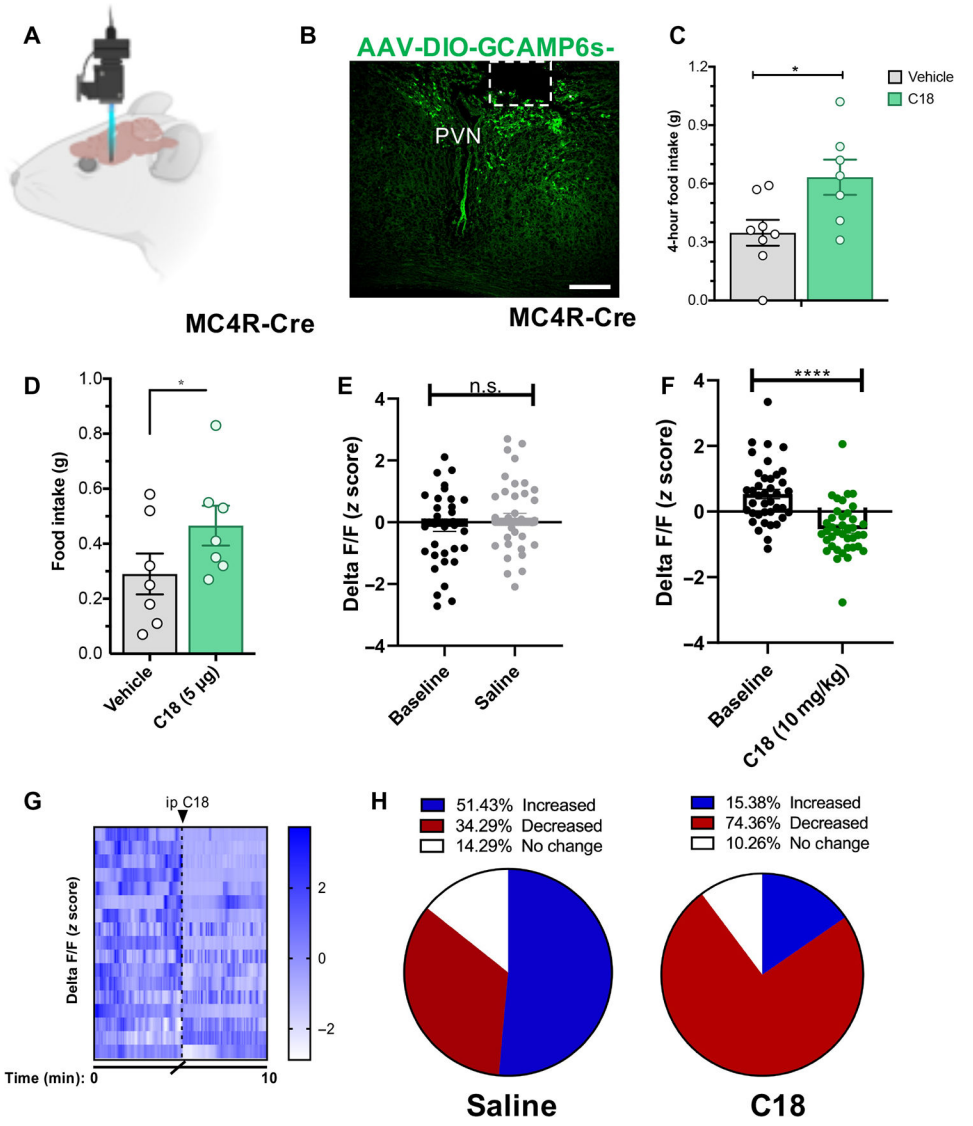

Fig. 8. MC3R agonism inhibits PVN MC4R neurons in vivo.

(**A**) Representative image depicting miniaturized microscope used for in vivo imaging studies. (**B**) Representative image showing expression of GCAMP6s in PVN MC4R neurons and lens placement in the PVN. Scale bar, 500 µm. (**C**) Four-hour food intake in WT mice after administration of the MC3R agonist C18 (10 mg/kg, ip) (n = 8 male mice for vehicle group and n = 7 male mice for C18 group). (**D**) Four-hour food intake after administration of vehicle (aCSF) or C18 (5 µg, 300 nl) into paraventricular hypothalamus (n = 7 male mice). (**E**) Change in fluorescence after intraperitoneal administration of saline (n = 3 male mice and 31 neurons). (**F**) Change in fluorescence after intraperitoneal administration of the MC3R agonist C18 (10 mg/kg, ip) (n = 3 male mice and 39 neurons). (**G**) Heat plot showing real-time change in fluorescence activity in a representative mouse during baseline and after administration of C18. (**H**) Pie chart showing distribution of neuronal responses after saline (left) or C18 administration (right). Data presented as means ± SEM in (C) to (F). (D) to (F)

analyzed with paired Student's *t* test. (C) analyzed with Student's unpaired Student's *t* test. $*P < 0.05$, $****P < 0.001$.